Hip imaging in athletes: sports imaging series

Agten, Christoph A ; Sutter, Reto ; Buck, Florian M ; Pfirrmann, Christian W A

Abstract: Hip or groin pain in athletes is common and clinical presentation is often nonspecific. Imaging is a very important diagnostic step in the work-up of athletes with hip pain. This review article provides an overview on hip biomechanics and discusses strategies for hip imaging modalities such as radiography, ultrasonography, computed tomography, and magnetic resonance (MR) imaging (MR arthrography and traction MR arthrography). The authors explain current concepts of femoroacetabular impingement and the problem of high prevalence of cam- and pincer-type morphology in asymptomatic persons. With the main focus on MR imaging, the authors present abnormalities of the hip joint and the surrounding soft tissues that can occur in athletes: intraarticular and extraarticular hip impingement syndromes, labral and cartilage disease, microinstability of the hip, myotendinous injuries, and athletic pubalgia.

DOI: https://doi.org/10.1148/radiol.2016151348

Radiology

Hip Imaging in Athletes: Sports Imaging Series[1]

Christoph A. Agten, MD
Reto Sutter, MD
Florian M. Buck, MD
Christian W. A. Pfirrmann, MD, MBA

Hip or groin pain in athletes is common and clinical presentation is often nonspecific. Imaging is a very important diagnostic step in the work-up of athletes with hip pain. This review article provides an overview on hip biomechanics and discusses strategies for hip imaging modalities such as radiography, ultrasonography, computed tomography, and magnetic resonance (MR) imaging (MR arthrography and traction MR arthrography). The authors explain current concepts of femoroacetabular impingement and the problem of high prevalence of cam- and pincer-type morphology in asymptomatic persons. With the main focus on MR imaging, the authors present abnormalities of the hip joint and the surrounding soft tissues that can occur in athletes: intraarticular and extraarticular hip impingement syndromes, labral and cartilage disease, microinstability of the hip, myotendinous injuries, and athletic pubalgia.

Online SA-CME
See www.rsna.org/education/search/ry

Learning Objectives:

After reading the article and taking the test, the reader will be able to:

- Describe biomechanical implications of torsional malalignment and other atypical forms of hip impingement
- Describe the most common MR imaging findings in femoroacetabular impingement and identify anatomic variants
- Describe imaging characteristics of a Morel-Lavallée lesion and identify the anatomic compartment where this lesion typically occurs
- Identify common stress fractures around the hip joint in athletes and discuss potential complications
- Describe features of myotendinous injuries around the hip
- Describe the anatomic relationship of the sacrotuberous ligament and the origin of the hamstring tendons
- Describe the anatomic structures involved in an athletic pubalgia

Accreditation and Designation Statement

The RSNA is accredited by the Accreditation Council for Continuing Medical Education (ACCME) to provide continuing medical education for physicians. The RSNA designates this journal-based SA-CME activity for a maximum of 1.0 *AMA PRA Category 1 Credit*™. Physicians should claim only the credit commensurate with the extent of their participation in the activity.

Disclosure Statement

The ACCME requires that the RSNA, as an accredited provider of CME, obtain signed disclosure statements from the authors, editors, and reviewers for this activity. For this journal-based CME activity, author disclosures are listed at the end of this article.

[1] From the Department of Radiology, Balgrist University Hospital, Forchstrasse 340, CH-8008 Zurich, Switzerland; and Faculty of Medicine, University of Zurich, Zurich, Switzerland. Received June 18, 2015; revision requested August 5; revision received September 8; accepted September 25; final version accepted October 20. **Address correspondence to** C.A.A. (e-mail: *christoph.agten@balgrist.ch*).

Hip or groin pain is common and is experienced by up to 23% of athletes during a 1-year period (1). Sports injuries depend on age and sex and the type of sport (eg, ballet, field-based sports, martial arts, running) (2). In children and adolescents, 10%–24% of sports-related injuries affect the hip (2,3) as opposed to about 5%–6% in adults (4). Table 1 provides frequencies of sports-related hip/groin injuries in professional athletes. In professional soccer players, overuse hip injuries are more common (73%) compared with acute injuries to the hip (27%) (5). The most common hip/groin injuries in soccer players are adductor injuries (64%), followed by hip flexor/iliopsoas injury (8%) (5). In National Football League athletes, common hip/groin injuries are muscle strains (59%) and contusions from direct impact (33%) (6). Intraarticular hip injuries in athletes are less frequent (6.2% in soccer and 5% in American football) (5,6). Time to full return to sport (days lost) is often one of the first questions asked by injured athletes. Mean number of days lost before return to sport in hip/groin injuries largely varies by injury type (Table 2).

Biomechanics

Biomechanical knowledge of the hip joint is important to understanding hip disease in athletes. Depending on the type of sports, fast acceleration and rotations can occur within the hip joint.

Bone

The hip joint is a ball-in-socket joint. Because of the high congruency of the femoral head and the acetabulum, most of the motion within the joint is rotational (7). Range of motion is limited by osseous structures. Insufficient osseous stability in the hip joint, as in a dysplastic hip, can lead to altered force transmission and damage to the joint (8). Abnormal bone contact as in patients with FAI or slipped capital femoral epiphysis is a cause for damage to the hip joint. Abnormal femoral torsion (angle between femoral condyles and femoral neck axis) is another factor for abnormal bone contact. A reduced femoral antetorsion can limit internal rotation with early bone contact, while an increased antetorsion limits external rotation (9). Patients with coxa valga combined with increased femoral antetorsion have reduced range of motion for extension, adduction, and external rotation and are reported to have a higher prevalence of extraarticular posterior impingement (10).

Cartilage

The hyaline cartilage covering the articular surfaces is important for force transmission in the joint (11). Direct impact to the greater trochanter leads to force transmission into the joint, which can result in focal cartilage defects on the femoral and acetabular side of the joint (12). Cartilage delamination at the acetabulum can occur in patients with a cam-type FAI owing to shear forces from the aspheric femoral head-neck junction (13).

Labrum

The labrum enlarges the acetabular surface by 22% (8). The labrum works as a seal to keep the joint fluid intraarticular and enhances joint lubrication, preventing cartilage wear (14). The labrum can be damaged by early contact between femur and labrum due to FAI (15) or during extreme hip motion (16). The labrum also assists in hip stability. Labral tears can lead to reduced stability in the joint because of loss of the sealing effect (16). Instability in the hip joint leads to translational motion in the joint and therefore shear forces in the cartilage and labrum (8).

Ligaments

The hip joint is further stabilized by multiple ligaments enhancing the joint capsule: the iliofemoral ligament (which is the strongest), the ischiofemoral ligament, the pubofemoral ligament, and the femoral arcuate ligament (also known as zona orbicularis) (17,18). The ligamentum teres, also known as the ligamentum capitis femoris, has gained more attention in recent years. Its main function is to limit hip rotation (19).

Muscles

Muscles around the hip also act as dynamic hip stabilizers. The iliocapsularis is one of the muscles that has been identified as stabilizer of the hip joint originating from the anteromedial joint capsule and inserting distally to the lesser trochanter (20). Marked hypertrophy and less fatty infiltration of the iliocapsularis muscle on magnetic resonance (MR) images is found in patients with dysplastic hips compared with patients with acetabular overcoverage (21).

Imaging Techniques

Radiography

After history and clinical examination, standard radiography is the first imaging modality to assess a painful hip. Standard radiographs are widely available and inexpensive. They provide a fast overview on the bone anatomy and many other abnormalities such as joint degeneration and fractures. The projections at our institution consist of a non–weight-bearing anteroposterior view of the pelvis and a cross-table lateral view

Essentials

- Knowledge of hip biomechanics helps in the understanding of sports-related hip disease.
- In athletes, labral tears are common findings that are often asymptomatic.
- In athletes with hip pain, periarticular structures need to be imaged because many abnormalities occur outside the hip joint.

Published online
10.1148/radiol.2016151348 **Content code:** MK

Radiology 2016; 280:351–369

Abbreviations:
AIIS = anterior inferior iliac spine
FAI = femoroacetabular impingement
FISP = fast imaging with steady-state precession
STIR = short tau inversion recovery
3D = three-dimensional
2D = two-dimensional

Conflicts of interest are listed at the end of this article.

Table 1

Frequency of Hip/Groin Injuries in Athletes

Sport	Frequency of Injuries Affecting the Hip/Groin	Most Common Injury Type in the Hip/Groin
Soccer (5,160)	12%–16%	Adductor/hamstring injuries
American football (6)	3.1%	Hip flexor strains
Basketball (174)	6.2%	Hamstring strains
Ice hockey (175,176)	4%–13.1%	Muscle-tendon strains (not specified)

Note.—Percentage of hip/groin injuries in relation to all injuries.

Table 2

Days Lost before Return to Sports per Hip/Groin Injury

Injury Type	Mean No. of Days Lost
Contusions	5.3 (1–30)
Muscle strains	8.9 (1–82)
Adductor injury	14 (1–197)
Labral tear	56–64 (3–127)
FAI	64 (NA)
Fracture	100.6 (65–184)

Note.—Numbers are mean days lost before full return to sports for American football (National Football League 1997–2006) and soccer (Union of European Football Associations 2001–2008) (5,6), with ranges in parentheses. FAI = femoroacetabular impingement, NA = not available.

of the affected hip. Other dedicated radiographic projections for hip assessment exist (eg, 45° Dunn view, 90° Dunn view, frog leg lateral view). The Dunn view (45°) projection especially provides good results regarding cam-type deformity using the alpha angle as criterion (22). However, cam deformity cannot definitely be excluded, even with dedicated radiographic projections.

A standardized and reproducible radiographic technique for the anteroposterior view of the pelvis is required. Subtle rotation and tilting of the pelvis can result in under- or overestimation of acetabular version (23). To avoid rotational malposition of the pelvis, the center of the sacrum needs to be vertically aligned with the symphysis. To avoid excessive tilting of the pelvis, the distance between the sacrococcygeal joint and the pubic symphysis should be around 32 mm for men and 47 mm for women in a standardized anteroposterior view of the pelvis (24). Software has been developed to correct for rotation and tilt by three-dimensional (3D) analysis of the two-dimensional (2D) images of the pelvis (25). Biplanar radiography with secondary 3D analysis can be used to assess femoral torsion (26) and calculate acetabular coverage (27).

Ultrasonography

Ultrasonography (US) is a valuable tool in the work-up of an athlete with hip pain (28). A major advantage of US is the possibility of dynamic evaluation of the hip, for example patients with snapping hip syndromes (29). Other advantages are accessibility on site at sporting events and relatively low cost. Commonly assessed structures are the iliopsoas tendon, iliopsoas bursa, and joint effusion. Evaluation of the acetabular labrum with US has been described (30). However, only the anterior part of the labrum is consistently seen, and other techniques such as MR arthrography are superior for detection of labral tears (31). Cam-type deformity anterosuperiorly can be detected with US, but with a low specificity (32). US is widely used for imaging-guided diagnostic or therapeutic injections around the hip joint. Because no radiation is used in US-guided injections, it is a valuable alternative to fluoroscopy-guided injections, especially in young athletes. Patients' satisfaction was reported to be higher with US-guidance compared with fluoroscopy for therapeutic hip injections (33).

Computed Tomography

Computed tomography (CT) is ideal for fracture analysis in blunt force trauma. However, CT has only limited value in evaluation of sports injuries in the hip. Three-dimensional CT can be used to assess bone morphology with respect to FAI (34). Dedicated software has been developed to assess virtual hip motion with 3D models from CT scans and visualize site of bone impingement (35). Labral tears and cartilage defects can also be detected at CT arthrography, but when the diagnostic performance is compared with that of MR arthrography, contradictory results have been reported (36,37). But as athletes with FAI are often young, CT with its ionizing radiation should be reserved for exceptional situations, such as patients with MR imaging contraindications.

MR Imaging

MR imaging is useful to assess intra- and extraarticular disease. Because hip/groin pain in athletes can have multiple origins, a dedicated hip imaging protocol is needed. Imaging is performed in a patient in the supine position with an empty bladder. To get an overview, a fluid-sensitive, fat-suppressed sequence in the coronal and/or transverse plane with a large field of view including the pubic symphysis is recommended to detect bone marrow and soft-tissue edema. Then a dedicated hip examination with a small field of view should be performed with a body matrix and surface coil. The imaged hip should be centered in the magnetic field.

A coronal T1-weighted turbo spin-echo sequence is helpful to assess bone marrow infiltration and fractures of the acetabulum or proximal femur. Fluid-sensitive sequences in the coronal plane help to detect bone marrow edema and nicely demonstrate anatomy of the ligamentum teres and the peritrochanteric region. Because of the spherical anatomy and the orientation of the acetabulum, standard imaging planes are susceptible to partial volume artifacts. Radial imaging improves the assessment of the complex 3D anatomy in hip imaging (38,39) and is part of the routine hip MR imaging and MR arthrography protocol at our institution (Table 3). Orientation of radial reformatted images is perpendicular to the transverse/short axis of the

Table 3

Hip MR Imaging and MR Arthrography Protocol

Parameter	Coronal T1-weighted TSE	Coronal Intermediate-weighted FS TSE	Oblique Transverse True FISP	Sagittal True FISP	Transverse T2-weighted HASTE: Hip	Transverse T2-weighted HASTE: Knee
Repetition time (msec)/echo time (msec)	600/13	2500/25	10.76/4.66	25.01/8.56	1000/93	1400/93
Section thickness (mm)	3	3	1	1.7	5	5
Field of view (mm)	180 × 180	180 × 180	170 × 170	159 × 159	240 × 240	240 × 240
Matrix	269 × 384	320 × 320	269 × 384	269 × 384	256 × 256	256 × 256
Echo train length	3	7	1	2	126	154
Pixel bandwidth (Hz/pixel)	130	130	200	130	700	700
No. of signals acquired	2	1	1	1	1	1
Acquisition time (min:sec)	3:39	3:57	4:15	4:22	0:25	0:14

Note.—Dedicated hip MR imaging and MR arthrography protocol for 1.5 T-MR machine (Magnetom Avanto-fit; Siemens Healthcare, Erlangen, Germany) used at the authors' institution. The identical parameters are used for MR imaging and MR arthrography. Leg traction is applied for MR arthrography studies (traction MR arthrography). Radial images perpendicular to the short axis of the femoral neck are reformatted from the oblique transverse true fast imaging with steady-state precession (FISP) sequence. The transverse T2-weighted HASTE sequences over the hip and knee are used to measure femoral antetorsion. FS = fat saturated, HASTE = half-Fourier acquisition single-shot turbo spin-echo, TSE = turbo spin echo.

femoral neck and neck-head junction, allowing assessment of the femoral neck-head junction at all positions, therefore improving detection of abnormalities such as cam-type deformity (39). Radial images can be acquired either directly planned on localizers (38,40) or secondary based on reformatting from a 3D isovoxel sequence (41). In one study, 3D imaging of the hip did not improve the diagnostic performance of cartilage lesions, but at least improved cartilage lesion conspicuity (42). In another study comparing 3D and 2D imaging, a lower specificity for detection of cartilage lesions was found for 3D, however accuracy for grading of cartilage lesions was higher using 3D sequences (43).

Role of MR arthrography.—Direct MR arthrography is superior to standard MR imaging in hip imaging for detection of labral and cartilage lesions (44). MR arthrography showed higher sensitivity compared with conventional MR imaging (69%–81% vs 50%) for detection of labral tears in the anterosuperior quadrant and a higher interreader agreement (44). MR arthrography also improved detection of acetabular cartilage defects, while no advantage was found for cartilage defects on the femoral head in comparison with conventional MR imaging (44).

For arthrography, the target zone for the needle is the center of the femoral neck or the superolateral quadrant of the femoral head (45). In patients who have undergone previous hip arthroscopy, the target zone is the superolateral femoral head because of possible adhesions between the joint capsule and the femoral neck, especially in patients who underwent osteochondroplasty of the femur (Fig 1).

Indirect MR arthrography has been reported as an alternative tool with a good detection rate for labral tears and cartilage disease (46).

It has been reported that 3-T standard MR imaging of the hip has the potential to replace 1.5-T MR arthrography because of the higher signal-to-noise ratio with 3-T imaging (47,48). However, in our opinion, dedicated coils and small field-of-view imaging are at least as important as field strength, resulting in very good image quality using new generation 1.5-T MR machines. Also, 3-T MR arthrography is of superior diagnostic quality compared with conventional 3-T MR imaging in the hip (49). Another advantage of MR arthrography over conventional MR imaging, regardless of field strength, is the possibility to distract the joint when continuous leg traction is applied.

Traction MR arthrography.—Distinction of the femoral and acetabular hyaline cartilage layer can be difficult at standard MR arthrography because no contrast is located between the layers. This limits the evaluation of the cartilage in the central hip compartment. MR imaging with continuous leg traction was first proposed 20 years ago (50). The combination of direct MR arthrography and leg traction was introduced in 2008 (51). Traction is usually achieved by using orthopedic traction devices. The weight used for traction varies: The mentioned study from 2008 used 6 kg (51). In one study using 8–10 kg for traction and an injected volume of 10–14 mL, joint distraction was achieved in only 8% (61 of 743) (52). In a recent study with direct MR arthrography using 15–23 kg of traction and an injected volume of 18–27 mL, a consistent separation of the acetabular and femoral cartilage layer could be achieved (53).

Cartilage delamination is especially difficult to see without traction, because the femoral head realigns the delaminated acetabular cartilage layer against the subchondral bone of the acetabulum. With adequate distraction, contrast agent can undermine the cartilage flap and therefore enhance visualization of cartilage delamination (54) (Fig 2). At our institution, traction MR arthrography is now routinely performed.

Athletic Hip and Groin Injuries

Stress Fractures and Avulsions

Stress fractures result from a mismatch between bone quality and mechanical

Figure 1

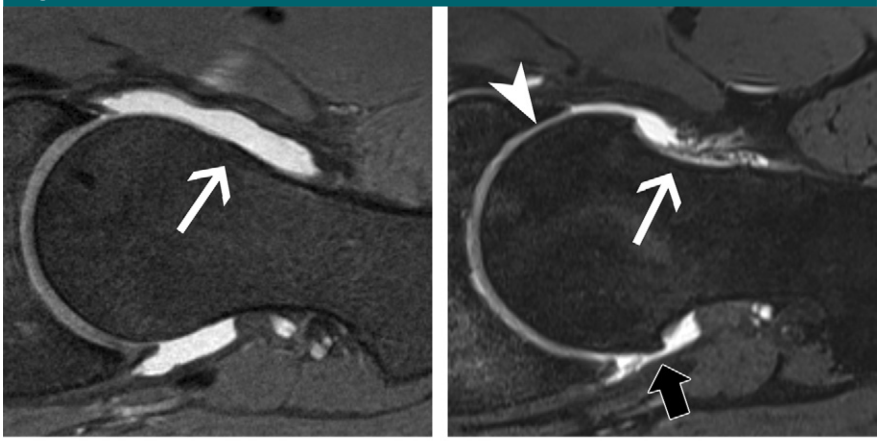

a. b.

Figure 1: MR images in a 22-year-old man with FAI **(a)** before and **(b)** 4 years after surgery. Oblique transverse water-excitation true FISP images (**a**, repetition time msec/echo time msec, 11.7/5.24; **b**, 11.02/4.3) of the left hip after direct arthrography: There is cam deformity anterosuperior/anterior (arrow, **a**). After osteochondroplasty at the head-neck junction there are capsular adhesions to the surgical site (white arrow, **b**). Note that the patient has undergone osteoarthritis changes in the meantime with osteophytes (black arrow) and cartilage thinning (arrowhead).

Figure 2

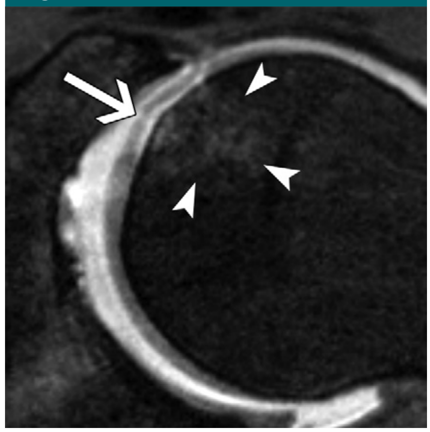

Figure 2: MR image in a 29-year-old elite floorball player with insidious, slowly increasing left-sided hip pain. On the oblique transverse water-excitation true FISP image (11.95/5.39) of the left hip after direct arthrography under leg traction with 22.5 kg, intraarticular contrast material is undermining the femoral cartilage (arrow), clearly delineating a large cartilage delamination and subchondral bone marrow edema (arrowheads). Without leg traction, this delamination would have been hard to detect.

stress to the bone. Stress fractures are usually divided into fatigue fractures (high stress, normal bone quality) or insufficiency fractures (normal stress, weak bone) (55). Stress fractures and fatigue fractures are often used as synonyms. In competitive track and field athletes, 21% of all athletes sustained a stress fracture in a 1-year period, with no difference between male and female athletes (56). However, young female athletes with risk factors called the "female athlete triad" (eating disorders, amenorrhea, and decreased bone density) have a cumulative higher risk for stress fractures with each of these risk factors—up to 20% for a single factor and 30%–50% for combined risk factors (57). Around the hip joint, common sites for stress fractures in athletes are the acetabulum and the femur. For acetabular stress fractures, two patterns have been described in endurance athletes: fractures in the acetabular roof and fractures in the anterior column (58). Femoral neck stress fractures are an important injury in runners (59). Medial femoral neck stress fractures result from repetitive compressive forces (compression-type stress fracture) and have a low risk for complications. Lateral femoral neck stress fractures have a higher risk for displacement (tension-type stress fracture) (60). After arthroscopic osteochondroplasty for cam deformity in FAI, insufficiency fractures of the femoral neck occur in about 2% of patients (61).

Radiographs have limited value for the detection of stress fractures and often no changes to the bone can be detected (62). Stress fractures may manifest on radiographs as horizontal bands or periosteal new bone formation only a few weeks after the onset of symptoms. MR imaging is much more sensitive than radiography or bone scintigraphy for the detection of stress fractures (63). Stress fractures on MR images manifest as bone marrow edema on fluid-sensitive images, typically with a hypointense line on T1-weighted, T2-weighted, and intermediate-weighted images (Fig 3). Bone marrow edema without a hypointense line may be referred to as a stress reaction instead of a stress fracture. Eventually a stress fracture develops if the mechanical stress to the bone persists. With healing of the stress fracture, the bone marrow edema disappears.

Avulsion fractures may result from an acute trauma or chronic repetitive stress and are usually seen in adolescents. Around the hip joint tendon avulsion fractures are most common. In adolescent athletes, common sites of avulsion fractures include the ischial tuberosity (hamstring tendons), anterior inferior iliac spine (AIIS) (direct head of the rectus femoris tendon, Fig 4), lesser trochanter (iliopsoas tendon), anterior superior iliac spine (tensor fascia latae and sartorius tendon), symphysis pubis (gracilis tendon), and the iliac crest (external oblique, internal oblique, and transverse abdominal muscles) (64). Avulsion fractures are common in sprinting, kicking, and gymnastics (64).

Bone marrow edema can be seen at the site of the avulsed fragment, but usually to a lesser extent when compared with classic fractures (65). The diagnosis of an avulsion fracture is sometimes difficult and the appearance on MR images and radiographs may even mimic a bone tumor, especially in chronic cases with bone overgrowth

Figure 3

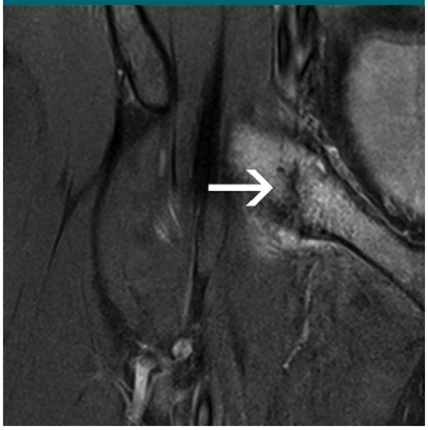

Figure 3: MR image in a 20-year-old man with hip pain and a clinically suspected labral tear. Coronal intermediate-weighted fat-saturated image (3550/39) of the right hip shows a stress fracture in the anterior column of the acetabulum. There is a vertically oriented hypointense fracture line (arrow) and marked bone marrow edema.

Figure 4

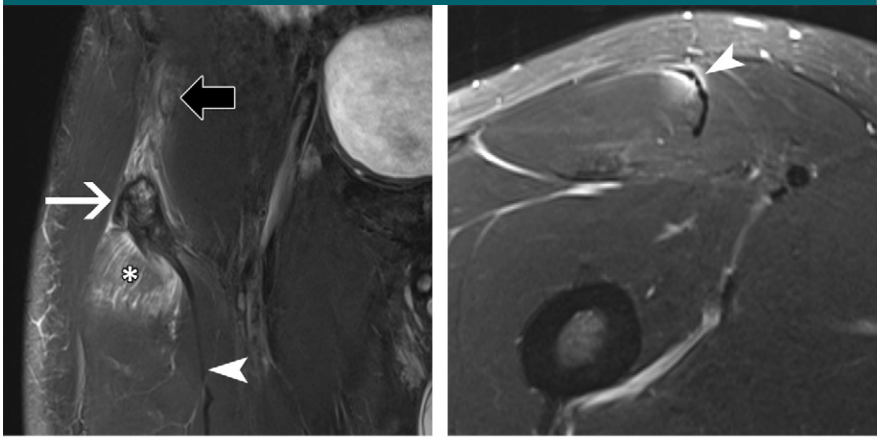

a. b.

Figure 4: MR images in a 29-year-old soccer player with hip trauma 2 weeks previous during play time. **(a)** Coronal (4000/59) and **(b)** transverse (5770/61) short tau inversion recovery (STIR) images show an osseous avulsion (white arrow) of the AIIS that is displaced distally. There is little bone marrow edema in the origin of the AIIS (black arrow). Note the feathery muscle edema (muscle strain) at the proximal myotendinous junction (*), extending far distally along the reflecting portion of the rectus femoris tendon (arrowhead).

(66). In avulsion fractures of the lesser trochanter in adults without a substantial traumatic event, metastatic disease should be suspected (67).

Impingement Syndromes of the Hip

Intraarticular Impingement

FAI is defined as an abnormal contact between the femur and the acetabulum, which may lead to early degenerative hip disease. Predisposing bone abnormalities that may lead to FAI are the pincer-type morphology (overcoverage of the acetabulum) and the cam-type morphology (deformity of the femoral head-neck junction) (41). A combination of pincer- and cam-type impingement (mixed-type FAI) is frequent and more common in male (62%) than female (32%) subjects (68). The clinical diagnosis is difficult. Impingement tests, such as the hip flexion-adduction-internal rotation test, show overall good sensitivity but lack sufficient specificity (69). The impingement test may even be positive in about 5%–7% of asymptomatic young adults (70).

Pincer-type FAI.—In pincer-type impingement, abnormal bony contact occurs between the acetabulum and the femur owing to a focal or general acetabular overcoverage. Focal acetabular overcoverage can be a result of an acetabular retroversion (71). General acetabular overcoverage is caused by an increased acetabular depth, as in coxa profunda and protrusio acetabuli (41). Acetabular depth can be measured on oblique transverse MR images as the distance between the femoral head center and the line connecting the anterior and posterior acetabular rim (41). On radiographs, three signs can help to detect acetabular retroversion: the crossover sign, the posterior wall sign, and the ischial spine sign (72). However, these signs are prone to intra- and interrater variability (73) and are susceptible to pelvic rotation and tilt on radiographs (74). One method to measure the acetabular version on transverse MR images is at the level of the acetabular roof as the angle between the line connecting the anterior and posterior acetabular rim and a vertical line (sagittal plane) (75). Another radiographic sign for pincer-type morphology is an increased lateral center-edge angle (> 40°) (68). An isolated pincer-type impingement, even in female subjects, is an uncommon finding, with mixed-type impingement being more common (68).

Cam-type FAI.—In cam-type impingement, an aspherical portion of the femoral head (the cam deformity) leads to abnormal bone contact and joint damage. Several theories exist as to how a cam deformity develops: Athletes in high-impact sports have a higher risk of developing a cam deformity of the femur (76). Very active participation in sports such as basketball, soccer, or American football before skeletal maturity may alter the development of the femoral physis and can result in a higher prevalence of cam deformity (77,78). Mechanical stimuli in vigorous sport activities can initiate an adaptive response at the femoral growth plate and therefore result in a cam deformity (79). In young soccer athletes, cam deformities gradually developed during skeletal growth over time in a 2-year follow-up (80).

Slipped capital femoral epiphysis alters the head-neck offset and the sphericity of the femoral head and therefore leads to FAI and early joint degeneration (Fig 5) (81). Slipped capital femoral epiphysis has been suggested to be one of the etiologic factors for cam-type impingement (82). Prevalence of a slip-like morphology in primary cam deformity was reported to be around 12%

Figure 5

Figure 5: MR image in a 14-year-old adolescent with bilateral slipped capital femoral epiphysis. Coronal T1-weighted image (605/13) of the left hip after direct arthrography shows medially slipped epiphysis and corresponding camlike deformity (arrow) at the femoral head-neck junction.

and differs from the idiopathic cam deformity (83). Two imaging signs are helpful to detect the slip-like morphology: the fovea sign and the tilt angle (83), both seen on radial MR images at the 2 o'clock anterosuperior position. The fovea sign is positive if the femoral neck axis does not cross the fovea capitis femoris. The tilt angle is calculated between the femoral neck axis and the line perpendicular to the connecting line between the two ends of the femoral epiphysis and is positive if the angle is greater than 4° (83). These signs may be more useful in research than in the clinical routine, as therapy is not different between idiopathic and slip-like cam deformities.

Other factors influencing the cam deformity are intrinsic factors such as sex and genetics (84). The relative risk for a cam deformity is increased 2.8-fold in siblings of patients with a known cam deformity and twofold for pincer deformity (85). Other risk factors for FAI include secondary deformities after Perthes disease (86) or posttraumatic conditions (87). In summary, the exact pathways for the development of cam deformities seem to be multifactorial and for the present time not completely understood.

Quantification of deformity and controversy on the alpha angle.—The alpha angle is the most commonly used method to quantify cam deformity. The alpha angle is defined as the angle between the long axis of the femoral neck through the center of the femoral head (line 1) and a line from the center of the femoral head through the point where the outer contour of the femoral head-neck junction crosses the circle with a radius of the cartilage-covered femoral head (line 2) (88). Classically the alpha angle has been used to quantify cam deformity anteriorly on angled axial MR images (88), and later the same method was used to quantify the cam deformity on radial reformatted MR images on multiple locations, as many cam deformities are present at the anterosuperior position (41). The classic cut-off angle for diagnosing a cam deformity was 55° initially, and it was recently suggested to be raised to 60° (89). The problem with the alpha angle and similar methods for quantifying cam deformity, such as the femoral offset and femoral distance, is the lack in discrimination between symptomatic and asymptomatic patients, limiting their clinical value (89,90).

Relevance of imaging findings.—The classic triad of MR imaging findings in cam-type impingement is made up of anterosuperior labral tears, anterosuperior cartilage defects, and cam-type morphology (eg, abnormal alpha angle) (91). FAI morphology is common in asymptomatic volunteers. Interestingly, the cam deformity is more prevalent in asymptomatic athletes (37%–55%) compared with the general asymptomatic population (23%) (92). This supports the theory that high-level sports activity is a factor for the development of clinically important FAI, at least in a subset of patients. Importantly, the clinical relevance of cam- and pincer-type morphology encountered at imaging should always be correlated with the clinical history and the physical examination. The presence of such deformities may predispose one to FAI. However, FAI is a dynamic process, which can only be diagnosed clinically including dynamic testing and not based on imaging alone.

Extraarticular Hip Impingement

Apart from the classic intraarticular FAI, other (less common) forms of hip impingement have been described (93).

Ischiofemoral impingement.—Ischiofemoral impingement is caused by impingement of soft tissues between the proximal femur and the ischium. MR imaging findings are edema in the quadratus femoris muscle, fatty atrophy of the quadratus femoris muscle, a narrowed ischiofemoral space (between ischium and lesser trochanter), a narrowed quadratus femoris space (between hamstring tendons and lesser trochanter), and, less frequently, involvement of the hamstring tendons (Fig 6) (94). In a recent meta-analysis, a cutoff of 15 mm or less for the ischiofemoral space (sensitivity, 76.9%; specificity, 81%) and 10 mm or less for the quadratus femoris space (sensitivity, 78.7%; specificity, 74.1%) was suggested (95). Pelvic morphology may also contribute to a narrowed ischiofemoral space. The intertuberous distance estimated by the ischial angle (between the horizontal plane and the ischiopubic ramus on transverse MR images) was reported to be higher in patients with ischiofemoral impingement compared with a control group (96). Ischiofemoral impingement is more common in women and older people (mean age, 50.8 years) (95). In asymptomatic elite gymnasts however, a narrowed ischiofemoral space and edema in the quadratus femoris muscle are frequent findings (up to 62.5%), often bilaterally (97).

Subspine impingement.—Subspine impingement is caused by soft-tissue impingement between the AIIS and the femur head-neck junction during hip flexion (98). Avulsion fractures of the AIIS in adolescent athletes are common and are also called sprinter's fractures (99). AIIS avulsions are frequent in soccer, tennis, and athletics (64). Healing of the avulsed fragment at a caudally dislocated position may result in an enlargement of the AIIS (Fig 7). The bone protuberance after a healed displaced

Figure 6

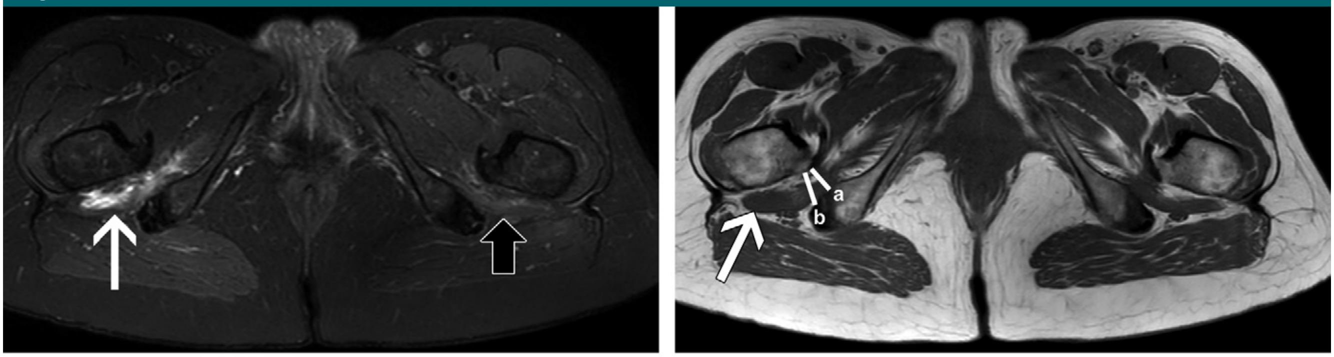

a. b.

Figure 6: MR images in a 55-year-old woman with symptomatic ischiofemoral impingement on the right side. **(a)** Transverse T2-weighted fat-suppressed image (4763/60) of the pelvis shows marked edema within the quadratus femoris muscle on the right side (white arrow) and only subtle edema (black arrow) on the left side. **(b)** The quadratus femoris muscle on the transverse T1-weighted image (714/7.45) shows no fatty infiltration or atrophy (arrow) and no narrowing of the ischiofemoral (distance *a*) and quadratus femoris space (distance *b*). CT-guided infiltration (not shown) with 1 mL triamcinolone 40 mg/mL and 1 mL ropivacain 0.2% using a 21-gauge needle into the quadratus femoris muscle on the right side yielded pain improvement (on a 0–10 visual analog scale: before infiltration, score of 7; 15 minutes after infiltration, score of 0.5).

Figure 7

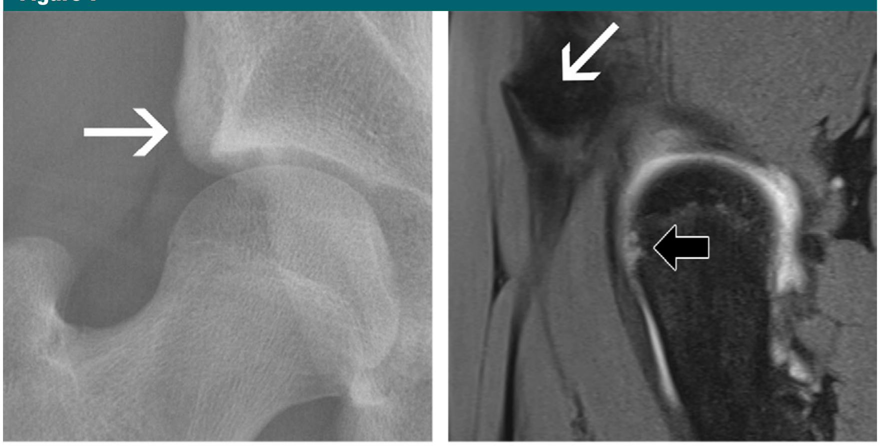

a. b.

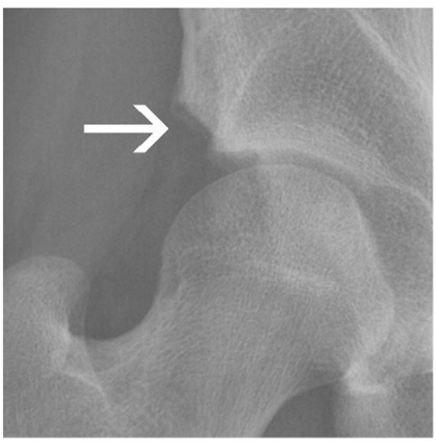

c.

Figure 7: Images in a 16-year-old male soccer player with hip pain of unclear origin for over 1.5 years. **(a)** Anteroposterior radiograph of the right hip shows a prominent AIIS (arrow). **(b)** Sagittal water-excitation true FISP image (25.01/8.56) of the right hip from direct MR arthrography shows osseous damage to the femoral head-neck junction (black arrow) and a prominent AIIS (white arrow), compatible with subspine impingement. **(c)** After surgical resection of the osseous prominence at the AIIS (arrow) the patient showed marked improvement of symptoms.

avulsion fracture of the AIIS is detectable on radiographs and especially with 3D CT with dynamic simulation (100).

Extreme hip motion.—Sports such as high-level martial arts, gymnastics, and ballet need a high range of motion in the hip. Extreme hip motion in end positions may result in a "pincer-like" impingement even with a normal bony morphology (101). MR imaging of elite female ballet dancers in the splits position showed a subluxation of the femoral head in this extreme position (101). Such incongruence in extreme hip positions may increase mechanical stress to the cartilage and labrum (101). Cartilage and labral damage in elite ballet dancers is more superior compared with nondancers, where it is more anterior (101).

Torsional malalignment.—An abnormal femoral torsion (angle on transverse CT or MR images between the line connecting the most posterior surface of both femoral condyles and the femoral neck long axis) is a factor for an FAI even in the absence of cam-type or pincer-type deformity (9). A reduced femoral torsion limits internal rotation and can lead to an early anterior bone impaction during internal hip rotation. An increased femoral torsion limits external rotation with early contact posteriorly (9). In asymptomatic volunteers mean femoral antetorsion has been reported as 12° with a standard deviation of 10° (9). Torsional abnormalities of the femur may occur independently or in combination with an increased or decreased acetabular version and should therefore be assessed separately (102).

Labrum

Acetabular labral tears are a frequent source of hip pain in athletes (103). Labral tears can occur in a variety of sports such as football, golf, and tennis (104). Known causes for labral tears are direct trauma, capsular laxity, dysplastic hip, and FAI (105). To describe the localization of labral tears there is a clock-face method, with 3 o'clock meaning anteriorly and 12 o'clock superiorly, regardless of laterality of the hip (106). Most acetabular labral tears (84%) are located anterosuperiorly, and 16% posterosuperiorly, while anteroinferior and posteroinferior tears are rare (44). Isolated anterior labral tears have been reported to be associated with iliopsoas impingement (107). At the anterosuperior position the labrum has biomechanical properties, such as lower compressive elastic modulus and lower tensile modulus compared with the other parts of the labrum, that favor tears at this location (108). Labral tears do not necessarily cause symptoms. A high prevalence (56%) of labral tears in asymptomatic hockey players has been reported (109). Of these players, only 14% developed hip symptoms within a 4-year follow-up period (110). Other investigators have found labral tears in asymptomatic volunteers in 69%–86% of studies (111,112). Therefore, interpretation of labral tears at MR imaging needs a clinical correlation.

Normal Variants

Several labral variants may be misdiagnosed as a labral tear. Sublabral recesses (also called sulci) are found arthroscopically in 18%–22% of patients (113,114). Typically, sublabral recesses are located anteroinferiorly at the 4 o'clock position, while labral tears are typically located anterosuperiorly (2 o'clock position) (114). Another frequent location for sublabral recesses is the posteroinferior location at the insertion of the transverse ligament (115). However, sublabral recesses can be found at all anatomic locations (116). Apart from localization, other criteria may be helpful to distinguish a recess from a labral tear: A recess is located at the base of the labrum, is linear in shape, and has smooth edges, while a tear often has irregular borders and may extend into the labral substance (117). Sublabral recesses do not extend through the full thickness of the labral substance and are not associated with paralabral cysts (Fig 8) (114,117).

Figure 8

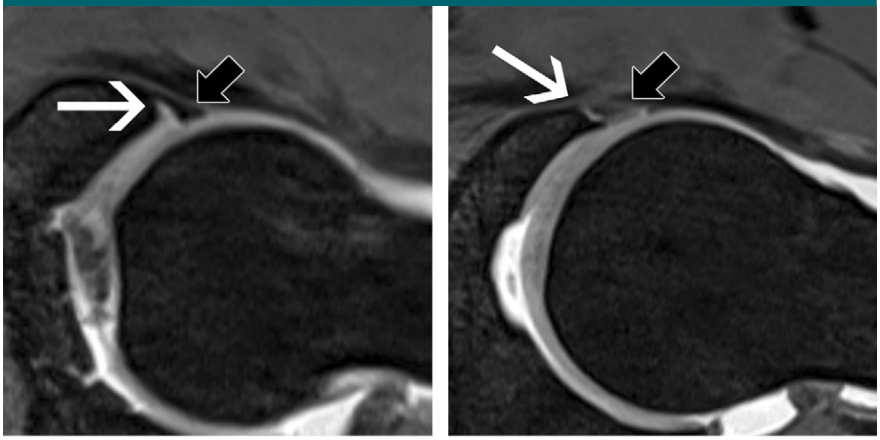

a. b.

Figure 8: MR images in a 26-year-old woman with sport-related hip pain and positive impingement tests on the left side. Oblique transverse water-excitation true FISP images (10.77/4.67) of the left hip after direct MR arthrography at the **(a)** anterior position 3 o'clock and **(b)** anterosuperior position 2 o'clock. The anterior sublabral recess (white arrow, **a**) is not completely separating labral base from the acetabulum, while the labral tear anterosuperiorly (white arrow, **b**) runs completely through the labrum base. Note the hypointensity of the normal labrum (black arrow, **a**) and the increased labral signal intensity of the labrum substance adjacent to the labral tear (black arrow, **b**).

At the capsular surface of the labrum, a perilabral recess between the joint capsule and the labrum exists. This perilabral recess is present circumferentially with variable depths, smallest at the superior position (118). It is usually not difficult to distinguish from a labral tear, but fluid or contrast material within the perilabral recess might mimic paralabral cysts.

Imaging Findings

Labral tears most commonly occur at the base of the labrum (detachment) or less frequently within the labrum substance as an intrasubstance tear (117)—most commonly at the anterosuperior position (44). About half of all labral tears are full-thickness tears (114). The torn labrum can show abnormal signal intensity and/or extension of contrast material into the labral substance (114). The presence of osseous abnormalities (cam deformity), cartilage damage, and paralabral cysts is associated with labral tears (114). In isolated pincer-type FAI the labrum typically shows thinning, intrasubstance fissuring, and fraying, while in cam-type FAI there is typically a chondrolabral avulsion (119).

Cartilage

Mechanism of Athletic Labral and Cartilage Injury

Acetabular and femoral cartilage damage may be caused by bone deformities (120). Shear forces to the cartilage caused by the eccentric portion of the femoral head in patients with cam deformities lead to cartilage delamination (13). In patients with cam deformities

Figure 9

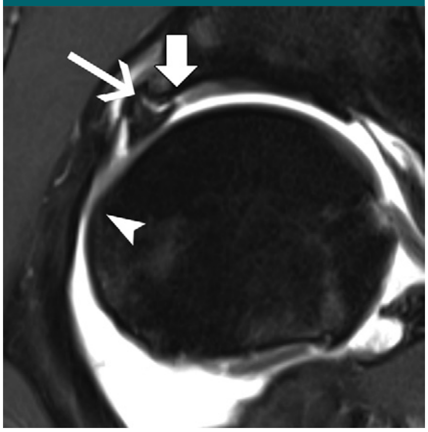

Figure 9: Image in a 27-year-old man with massive right-sided groin pain. Coronal intermediate-weighted fat saturated direct MR arthrography image (2800/33) of the right hip with hip traction. Labral tear (white arrow) with adjacent cartilage delamination (black arrow) in a patient with cam-type deformity (arrowhead)—the classic triad of imaging findings in cam-type impingement.

Figure 11

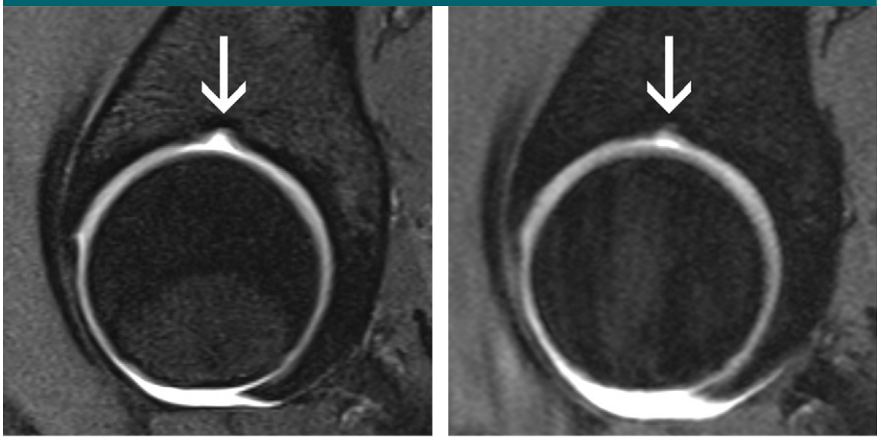

a. b.

Figure 11: MR images in an 18-year-old woman with hip pain. **(a)** Sagittal intermediate-weighted fat-saturated image (2600/32) of the right hip after direct arthrography show supraacetabular fossa type 1 (arrow). **(b)** Sagittal water-excitation true FISP MR image (25.16/8.56) obtained at follow-up 8 months later shows a supraacetabular fossa type 2 at the same location, indicating the physiologic progression of this normal variant, as the fossa is getting smaller and is now filled with cartilage (arrow). This should not be mistaken for an osteochondral lesion.

Figure 10

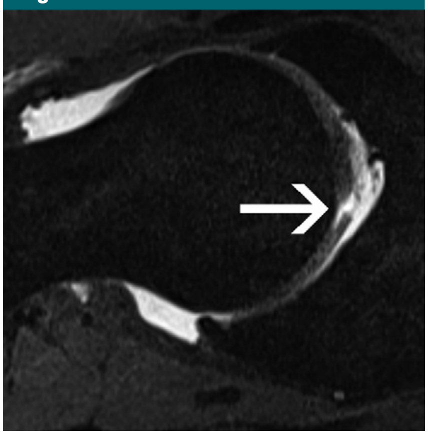

Figure 10: MR image in a 28-year-old professional male ice hockey player with hip pain for 2 weeks after a sudden pain event on ice. Oblique transverse water-excitation true FISP MR image (11.02/4.3) of the right hip after direct MR arthrography without traction shows a parafoveal cartilage delamination on the femoral head (arrow).

of the femoral head, cartilage delamination is a frequent finding (44%–52%), most often located directly adjacent to labral tears (Fig 9) (13,121). Therefore, cartilage defects in FAI are typically located anterosuperiorly (122). Acetabular overcoverage may have some protective effect against cartilage delamination (121). In pincer-type FAI, cartilage lesions are also found in the posteroinferior part of the acetabulum (41).

In athletes, direct impact injury can lead to acetabular and/or femoral cartilage defects (123). Parafoveal cartilage defects posterosuperiorly on the femoral head have been described in active patients with cam-type impingement participating in activities requiring repetitive, fast, and forceful hip flexion, such as martial arts, American football, hurdles, and soccer (Fig 10) (124).

Normal Variants

A supraacetabular fossa in the acetabular roof (12 o'clock) is an anatomic variant present in about 10% of individuals (125). The fossa can be a defect in the subchondral bone and cartilage, filled with joint fluid (type 1), or only in the subchondral bone, filled with cartilage (type 2) (125). A supraacetabular fossa is distinct from the acetabular fossa and probably represents an age-related developmental morphologic variation, with type 1 supraacetabular fossa undergoing remodeling over time, appearing as a type 2 supraacetabular fossa (Fig 11) (125). A supraacetabular fossa should not be mistaken as an osteochondral defect.

Another variant is the superior acetabular roof notch, which is a sharply delineated, more longitudinally, fluid- or fat-filled pit in the medial aspect of the acetabular roof, distinct from the supraacetabular fossa (Fig 12) (125). On radiographs, a superior acetabular roof notch is present in 17% of men and 22% of women (126). The stellate lesion, also called stellate crease, is another anatomic variant of the acetabulum seen at arthroscopy. A stellate lesion is an area of the acetabular roof without cartilage coverage, located more medially than a supraacetabular fossa. Data on this lesion are limited (127). Some authors believe it is a residuum of a healed supraacetabular fossa or a healed roof notch, as it is placed a bit more medially than the supraacetabular fossa (128).

Imaging Findings

Cartilage defects can be described as focal defects or thinning (44). On MR arthrography images, cartilage defects may fill up with injected contrast material. Increased signal intensity of the

Figure 12

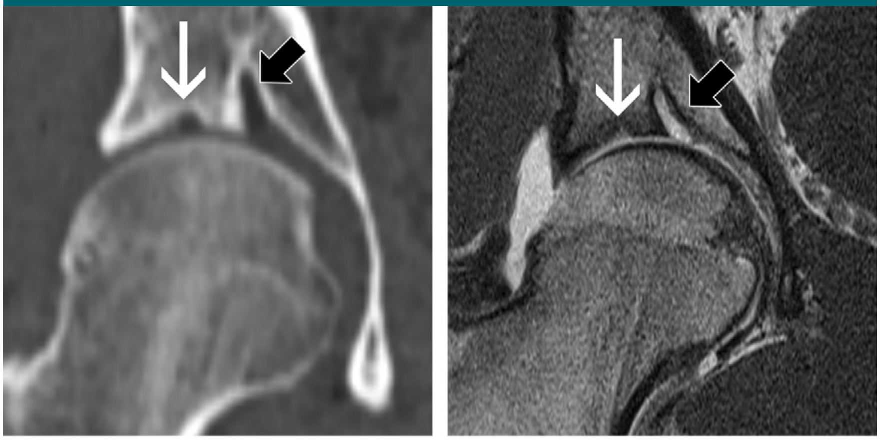

a. b.

Figure 12: Images in an 18-year-old man with previous arthroscopy of the right hip due to FAI. **(a)** Coronal CT reconstruction and **(b)** coronal T1-weighted MR image (608/13) of the right hip both show a supraacetabular fossa (type 2) (white arrow) and superior acetabular roof notch (black arrow) in the same patient. These findings were bilateral (left side not shown). The superior acetabular roof notch is filled with fat tissue.

Figure 13

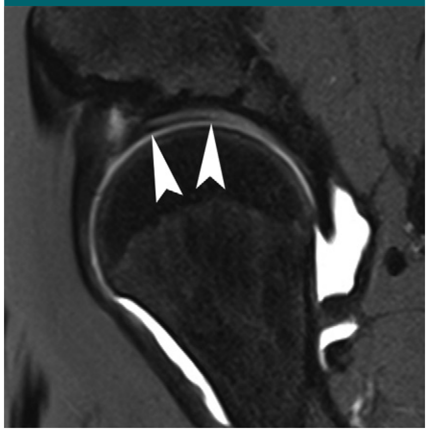

Figure 13: MR image in 22-year-old man with recurrent hip pain on the right side. Sagittal intermediate-weighted fat-saturated image (2882.1/33) of the right hip shows a linear hypointensity in the acetabular cartilage (between arrowheads), consistent with cartilage delamination. A phenomenon of "carpet delamination" was reported during a hip arthroscopy at this location 18 months earlier but was not surgically addressed.

cartilage may lead to overestimation and false-positive cartilage defects (122). Fluid or injected contrast material undermining the cartilage layer is a specific (however, not sensitive) sign for cartilage delamination (13). On intermediate-weighted fat-saturated and T1-weighted MR arthrography images, a hypointense signal intensity within the normally intermediate intensity acetabular cartilage is a helpful sign with high specificity (90%–95%) for cartilage delamination detection (Fig 13) (13). However, these signs lack a good sensitivity (22%–74%) for cartilage delamination (13).

Multiple quantitative techniques have been applied to the hip for cartilage mapping: delayed gadolinium-enhanced MR imaging of cartilage (dGEMRIC), T2*-, and T1ρ-mapping. dGEMRIC for cartilage assessment in patients with FAI showed only a weak correlation with intraoperative findings (129). Cartilage mapping is not routinely performed at our institution and its clinical impact has yet to be established.

Instability of the Hip Joint

Concept and Controversies

Because of the osseous congruency and the depth of the acetabulum, the hip is an intrinsically stable joint. The surrounding soft tissues such as the labrum, joint capsule, ligaments, and muscles are important static and dynamic hip stabilizers in sports (130). In a lax hip during motion, the joint and its surrounding soft tissues are suspected to not be capable of keeping the femoral head centered in the acetabulum (130). The concept of microinstability is based on symptomatic hip laxity, but without complete luxation or marked subluxation (130). Origin of microinstability is believed to be either traumatic (single or repetitive trauma) or atraumatic (generalized laxity or developmental dysplasia of the hip). The clinical diagnosis is difficult, as there are no clear criteria for hip microinstability (52). Patients may feel "instability" in the hip joint, snapping, and/or pain during sports (130). If conservative treatment fails, hip arthroscopy may be performed by some surgeons to reduce capsule volume (131).

Role of Imaging

In patients with suspected microinstability, radiographs can reveal underlying developmental dysplasia of the hip. Another reason may be that the aspheric head which is present with cam deformities may lead to leverage of the head out of the socket and thus to microinstability (52). On MR images, a thickened iliofemoral ligament (anterior joint capsule) with irregularities on the undersurface of the anterior capsule has been described as a sign correlating with clinical findings of laxity (130). However, a contradicting study reports an anterior capsular thinning in hip laxity (2.5 mm with laxity versus 3.3 mm without laxity) (132). Patients with microinstability may be suspected to have an increased capsule volume, which might be detected during arthrography. Traction MR arthrography sometimes shows larger widening of a hip joint, potentially indicating hip laxity. Patients with a successful joint distraction at traction MR arthrography with a relatively low weight of 8–10 kg showed smaller center edge angles compared with those with unsuccessful joint distraction (52). Other findings associated with positive joint distraction were higher alpha angles, higher neck-shaft angles, smaller acetabular depths, and hypertrophy of the ligamentum teres (52).

Ligamentum Teres

The ligamentum teres is an external rotation stabilizer and has gained more attention in recent years (133). The ligamentum teres has a broad origin in the acetabular fossa with two bands blending in with the transverse ligament and inserts in the fovea capitis femoris (134). Ligamentum teres injuries are a possible source of hip pain and may respond to arthroscopic treatment (135). Arthroscopically ligamentum teres lesions are categorized as complete rupture, partial rupture, or degeneration (136). The ligament is completely torn after frank hip dislocation, but tears may also occur with sudden external rotation (137). On MR images, the normal ligamentum teres has smooth borders and a homogeneous, hypointense structure at all sequences (137). The ligament is best visualized in the coronal and transverse plane (also oblique transverse). Ligament degeneration is similar to tendons, ranging from mucoid degeneration to complete tears (138). Complete tears are most commonly located near the fovea and show a discontinuity of the ligament with lax contours (Fig 14) (130,137). MR imaging (67% sensitivity, 99% specificity) and MR arthrography (67% sensitivity, 100% specificity) show similar good results for the detection of complete tears, with hip arthroscopy as reference standard (139). However, MR arthrography offers a better diagnostic performance compared with MR imaging regarding partial tears (139).

Myotendinous Injuries around the Hip Joint

Tendon injuries are often overuse injuries or a result of a single traumatic event. At MR imaging, tendinopathic tendons are thickened and show increased signal intensity on T1-weighted images. In partial tears, fluid-filled defects within the tendon substance can be detected on fluid-sensitive MR images such as STIR, T2-weighted, and intermediate-weighted fat-saturated images. Full-thickness tears show a complete discontinuity of the tendon with various degrees of tendon retraction (140).

Abductor Tendons

The greater trochanteric pain syndrome refers to peritrochanteric pain with abnormalities of the hip abductor tendons and the greater trochanteric bursa. It is a common cause for lateral hip pain in active middle-aged women (141). Apart from a trochanteric bursitis, the abductor tendons (gluteus minimus and gluteus medius tendon) can be affected. Peritendinitis is the earliest manifestation of tendon damage and manifests as fluidlike signal intensity superficial to the tendon (142).

Athletes, especially runners, dancers, soccer players, and weight lifters, may encounter an external snapping hip syndrome, with popping movements of the iliotibial band or the gluteus maximus muscle over the greater trochanter during full extension of the hip (143). Such an external snapping hip is primarily a clinical diagnosis (144). US can show in real time the sudden displacement of the iliotibial band or gluteus maximus muscle over the greater trochanter and fluid in the trochanteric bursa (145). Other US findings are a hypoechoic and thickened iliotibial band at the level of the greater trochanter (145). Reactive fluid within the trochanteric bursa from repetitive mechanical snapping can easily be identified on MR images between the gluteus medius tendon and the gluteus maximus muscle/iliotibial band, sometimes extending posterior around the greater trochanter (144). On MR images the iliotibial band may be thickened with adjacent soft-tissue edema (144).

Morel-Lavallée Lesion

A different entity from trochanteric bursitis is the Morel-Lavallée lesion. It is a posttraumatic, typically encapsulated fluid collection between the superficial and deep fascia layers of the lateral thigh, classically in the trochanteric region adjacent to the fascia lata (Fig 15) (146). As a result of severe shearing forces or compression (closed degloving injury), vessels perforating the different fascia layers are damaged and leak into the virtual space between the superficial and deep fascia. Because the Morel-Lavallée lesion is encapsulated, it does not resolve spontaneously and usually requires surgical treatment or drainage (147). If chronic, it may mimic a soft-tissue mass (eg, sarcoma) (148). An MR classification system for Morel-Lavallée lesions has been proposed (types I–V), depending on morphology, capsule, T1 and T2 signal intensity, and contrast enhancement (146).

Figure 14

Figure 14: MR image in a 28-year-old professional female ballet dancer with hip pain. Coronal intermediate-weighted fat-saturated image (2800/33) after direct arthrography shows a full-thickness rupture of the ligamentum teres (white arrow). Normal ligamentum teres anatomy is shown in inlay figure of a different 20-year-old male patient with internal snapping hip syndrome (black arrow).

Iliopsoas Tendon

The internal (extraarticular) snapping hip syndrome is caused by sudden movements of the iliopsoas tendon over the iliopectineal eminence, the femoral head, a paralabral cyst, over the medial aspect of the iliacus muscle itself, or over a bifid iliopsoas tendon (144,149). Snapping of the iliopsoas tendon can be accompanied by an iliopsoas tendinopathy and iliopsoas bursitis, both detectable at MR imaging and US (150,151). Iliopsoas tendinopathy is an underrecognized source

Figure 15

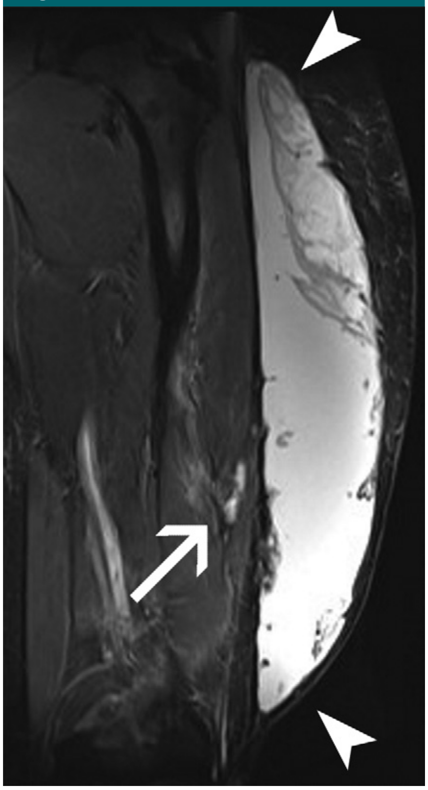

Figure 15: MR image in a 30-year-old man after a contusion to the left thigh 3 weeks previously. Coronal STIR image (4420/39) of the left thigh shows a massive, encapsulated hematoma between the deep and superficial fascial layers (Morel-Lavallée lesion, arrowheads), reaching from the greater trochanter down to the femoral condyles. In addition, there is a small intramuscular hematoma in the vastus lateralis and intermedius muscles (arrow).

Figure 16

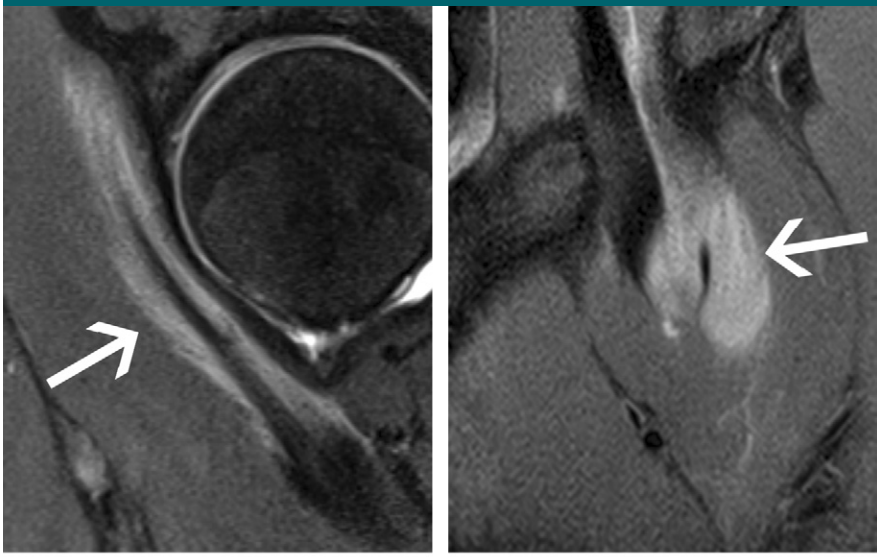

a. b.

Figure 16: MR images in a 16-year-old male patient with previous abduction trauma of the left hip and subsequent clinical hip impingement. **(a)** Sagittal and **(b)** coronal intermediate-weighted fat-saturated images (2750/31) after direct arthrography show feathery edema along the iliacus tendon (muscle strain injury to the myotendinous junction; arrow).

of hip pain in athletes, especially in high-energy sports such as soccer or ice hockey (152). Imaging findings of iliopsoas tendinopathy include a thickened tendon and high signal intensity on images obtained with fluid-sensitive sequences (152). Fluoroscopically or US-guided iliopsoas bursa injections with local anesthetic and corticosteroids are diagnostic and/or therapeutic options in suspected iliopsoas tendinopathy, with a benefit reported in 72% of patients (153,154). Iliopsoas tendon tears usually occur at the tendinous portion, while the muscular insertion of the iliacus muscle remains intact (155). In an acute full-thickness tear, adjacent soft-tissue edema and hematoma are often present (Fig 16). In chronic cases, an iliopsoas bursitis is a common finding (152).

Rectus Femoris Tendon

The rectus femoris tendon origin has two components, a direct head originating from the AIIS and a reflected (indirect) head origination from the lateral aspect of the acetabulum, both fusing to one tendon shortly below the AIIS (156). Rectus femoris tendon tears manifest as acute injuries, typically in soccer players, American football players, and sprinters (157). However, myotendinous strains of the reflected tendon may have an insidious presentation (157). Proximal tendon injuries, partial tears, and complete tears can be depicted with transverse MR imaging sequences, but the extent and the retraction is better visualized in the sagittal or oblique sagittal plane. Injuries of the reflected (indirect) head of the rectus femoris are more common than injuries of the direct head (158). The myotendinous junction of the reflected (indirect) tendon part is quite long, and myotendinous injuries of the reflected tendon can reach far distally into the thigh (Fig 4) (157).

Hamstrings

The biceps femoris muscle, the semitendinosus muscle, and the semimembranosus muscle form the hamstring muscle complex, originating from the ischial tuberosity. The biceps femoris tendon and the semitendinosus tendon originate as a conjoint tendon posteromedial to the semimembranosus tendon. Hamstring injuries occur at the weakest link in the bone-tendon-muscle unit: ischial tuberosity bone avulsions in children, myotendinous junction injuries in adolescent and young athletes, and injuries of the tendon itself in older adults (159). In professional soccer players, hamstring muscle strains are the most common single injury subtype and are clinically severe (>28 days lost from playing sports) in 15% of patients (160). The return to play time in hamstring injuries correlates with a simple MR imaging classification system (grade 0 = negative at MR imaging, grade 1 = edema, grade 2 = partial tear, grade 3 = muscle or tendon rupture) (161). Because return

Figure 17

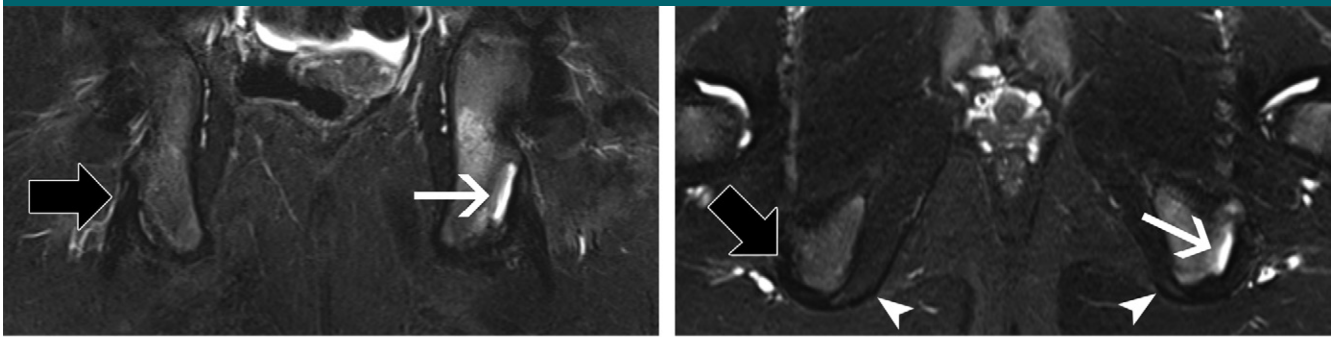

a. b.

Figure 17: MR images in a 12-year-old female patient competing in gymnastics on international level with left-sided gluteal pain. **(a)** Coronal and **(b)** transverse STIR images (4000/60) of the pelvis show a partial tear of the left hamstring tendon origin with fluid between tendon and bone (white arrow). Hamstrings on the right side are normal (black arrow). Note the sacrotuberous ligament (arrowheads).

to play time within a single grade can show large variations and overlap with other grades, the prognostic value for the individual athlete is limited. A more comprehensive MR imaging classification system for hamstring injuries has been recently proposed (the British Athletics Muscle Injury Classification) (162). With this new classification system, injuries are classified not only with respect to extent but also location of injury within the muscle (myofascial, myotendinous, intratendinous) (162).

Over 50% of hamstring injuries occur in the biceps femoris (163). Proximal hamstring tendinopathy is difficult to diagnose on MR images. Increased signal intensity in the proximal hamstring tendon on T1- and T2-weighted images is very common in patients with and those without clinical symptoms of hamstring tendinopathy (164). Ischial tuberosity edema is a frequent MR imaging finding in patients with symptomatic hamstring tendinopathy (odds ratio, 6.99) (164). Other suggestive findings are peritendinous edema with a feathery appearance in muscles and an increased thickness of the hamstring tendons (164). In partial-thickness hamstring tendon tears, fluid partially separates the tendon origin from the ischial tuberosity (Fig 17), while in full-thickness tears, the tendon shows a complete detachment and retraction (165). Surgical treatment in athletes with partial tears should be reserved for failed nonsurgical treatment (166). An interesting anatomic observation is the continuity of the sacrotuberous ligament with the ischium and the conjoint tendon (biceps femoris and semitendinosus) but not with the semimembranosus tendon (165). In a hamstring tendon tear with an intact sacrotuberous ligament, less retraction of the torn tendon is observed (165).

External Rotators

There are limited data on sports-related injuries to the short external rotator tendons (piriformis, internal and external obturator). Muscle strains to the external rotator muscles in American football are uncommon (6% of all muscle strains around hip joint), but interestingly resulted in significantly more days lost before return to play compared with other muscle strains (6).

Athletic Pubalgia

Athletic pubalgia accounts for about 4% of groin injuries in professional soccer players (5). The term *athletic pubalgia* is defined as chronic groin pain during activity (167). This pain syndrome has formerly also been called "sports hernia," however this is a misleading term, since no hernia is present. The clinical term *athletic pubalgia* comprises multiple causes affecting the pubic symphysis region: injuries to the rectus abdominis insertion, origin of the hip adductor tendons, and the pubic symphysis (167).

Anatomy

The pubic symphysis is formed by the two pubic bones with hyaline cartilage on opposing articulating surfaces, separated by a fibrocartilage disc. The physiologic joint space of the pubic symphysis is also termed the primary cleft. The pubic symphysis is supported by four ligaments (anterior, posterior, superior, and inferior [arcuate] ligament). Some of these ligaments are contiguous with the disc, the surrounding muscle attachments, and muscle origins, supporting overall stability (168). This leads to a prominent aponeurotic plate, connecting the distal rectus abdominis attachment, the pubic symphysis, and the adductor longus origin. Close anatomic proximity of these structures with the medial border of the superficial inguinal ring may explain inguinal hernia–like symptoms in patients with athletic pubalgia, even though true hernias are absent in these patients (169).

Tendon and Bone Injury

Tears of the aponeurosis connecting the rectus abdominis and the adductor longus muscle can be detected on fluid-sensitive MR images as fluidlike areas undermining the aponeurosis (170). Sagittal and coronal oblique planes (perpendicular to the aponeurosis) with a small field of view are recommended (171). In case of an injury, separation of the aponeurotic plate from the pubic bone inferolateral forms a secondary

Figure 18

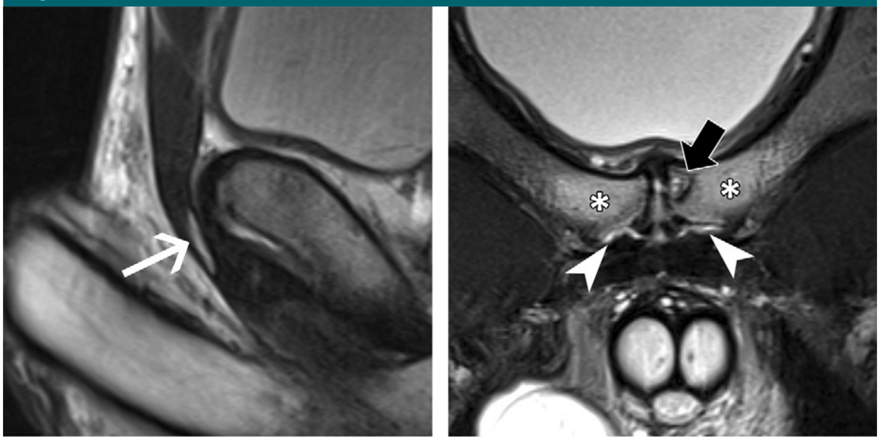

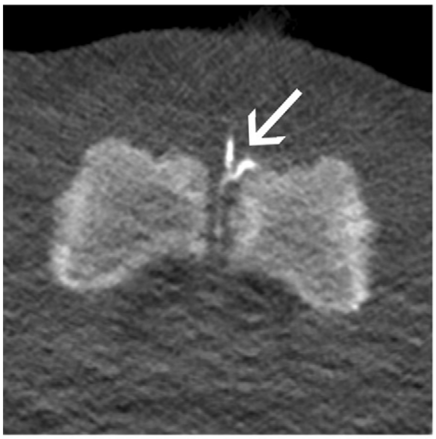

Figure 18: Images in a 20-year-old professional soccer player with groin pain on both sides (pain on left more than right). **(a)** Sagittal T2-weighted image (3040/85) shows a partial tear in the aponeurotic plate of the rectus abdominis muscle (arrow). **(b)** Oblique coronal STIR image (5000/61) confirms partial tear in the aponeurotic plate (arrowheads). There is bilateral marked bone marrow edema (*) and a small erosion in the left pubic bone (black arrow), confirming an osteitis pubis. **(c)** CT-guided pubic symphysis infiltration with 0.5 mL triamcinolone (40 mg/mL) and 0.5 mL rapidocaine 2% shows tip of the needle and a secondary cleft on the left side (arrow). The patient was pain free 15 minutes after the infiltration.

cleft, which contains fluid on fluid-sensitive MR images (Fig 18) (170). However, this so-called secondary cleft sign only has moderate sensitivity (57%) and specificity (60%) for diagnosing injury of the aponeurosis (169). Recently, a superior cleft sign has been described as a sign for tearing of the rectus abdominis/adductor longus junction more cranially (172). The superior cleft sign is positive if fluid on MR images or injected contrast material at symphysography linearly leaks parallel to the inferior margin of the superior pubic ramus to the side of symptoms (172).

A more obvious finding is frank tendon avulsion from the pubic bone (173). Associated bone marrow edema anteroinferiorly in the pubic bones is common and was reported in over 50% of patients with athletic pubalgia (169). Other imaging signs are edema or atrophy of the rectus abdominis muscle attachment. Thickening or increased signal intensity of the adductor tendon origins, reflecting adductor tendinopathy, is often associated with aponeurotic tears (173).

While acute injury of the aponeurosis is commonly seen in athletes, the pubic symphysis may also show chronic changes: Osteitis pubis manifests as osseous irregularities of the pubic symphysis with erosions, productive changes such as sclerosis and osteophytes. Osteitis pubis may be present without damage to the aponeurotic plate (169).

Involvement of rectus abdominis attachment, the adductor origin, pubic symphysis articulation (osteitis pubis), or any combinations should be stated in MR reports, as treatment may be different (169).

Summary

We described sports-related anatomy, biomechanics, and disease of the hip joint with special focus on MR imaging. The high prevalence of "pathologic" findings in asymptomatic athletes mandates the need for close communication between radiologists and the referring clinical colleagues. The often nonspecific clinical presentation of athletes with hip and/or groin pain requires a thorough evaluation of the hip joint itself on MR images, but the surrounding soft tissues are equally important.

Disclosures of Conflicts of Interest: C.A.A. disclosed no relevant relationships. **R.S.** disclosed no relevant relationships. **F.M.B.** disclosed no relevant relationships. **C.W.A.P.** disclosed no relevant relationships.

References

1. Jonasson P, Halldin K, Karlsson J, et al. Prevalence of joint-related pain in the extremities and spine in five groups of top athletes. Knee Surg Sports Traumatol Arthrosc 2011;19(9):1540–1546.
2. Stracciolini A, Casciano R, Levey Friedman H, Meehan WP 3rd, Micheli LJ. Pediatric sports injuries: an age comparison of children versus adolescents. Am J Sports Med 2013;41(8):1922–1929.
3. Boyd KT, Peirce NS, Batt ME. Common hip injuries in sport. Sports Med 1997;24(4): 273–288.
4. Braly BA, Beall DP, Martin HD. Clinical examination of the athletic hip. Clin Sports Med 2006;25(2):199–210, vii.
5. Werner J, Hägglund M, Waldén M, Ekstrand J. UEFA injury study: a prospective study of hip and groin injuries in professional football over seven consecutive seasons. Br J Sports Med 2009;43(13): 1036–1040.
6. Feeley BT, Powell JW, Muller MS, Barnes RP, Warren RF, Kelly BT. Hip injuries and labral tears in the national football league. Am J Sports Med 2008;36(11): 2187–2195.
7. Harding L, Barbe M, Shepard K, et al. Posterior-anterior glide of the femoral head in the acetabulum: a cadaver study. J Orthop Sports Phys Ther 2003;33(3):118–125.

8. Bowman KF Jr, Fox J, Sekiya JK. A clinically relevant review of hip biomechanics. Arthroscopy 2010;26(8):1118–1129.

9. Sutter R, Dietrich TJ, Zingg PO, Pfirrmann CW. Femoral antetorsion: comparing asymptomatic volunteers and patients with femoroacetabular impingement. Radiology 2012;263(2):475–483.

10. Siebenrock KA, Steppacher SD, Haefeli PC, Schwab JM, Tannast M. Valgus hip with high antetorsion causes pain through posterior extraarticular FAI. Clin Orthop Relat Res 2013;471(12):3774–3780.

11. Daniel M, Iglic A, Kralj-Iglic V. The shape of acetabular cartilage optimizes hip contact stress distribution. J Anat 2005;207(1):85–91.

12. Byrd JW. Lateral impact injury: a source of occult hip pathology. Clin Sports Med 2001;20(4):801–815.

13. Pfirrmann CW, Duc SR, Zanetti M, Dora C, Hodler J. MR arthrography of acetabular cartilage delamination in femoroacetabular cam impingement. Radiology 2008;249(1):236–241.

14. Ferguson SJ, Bryant JT, Ganz R, Ito K. An in vitro investigation of the acetabular labral seal in hip joint mechanics. J Biomech 2003;36(2):171–178.

15. Kapron AL, Aoki SK, Peters CL, Anderson AE. Subject-specific patterns of femur-labrum contact are complex and vary in asymptomatic hips and hips with femoroacetabular impingement. Clin Orthop Relat Res 2014;472(12):3912–3922.

16. Crawford MJ, Dy CJ, Alexander JW, et al. The 2007 Frank Stinchfield Award: the biomechanics of the hip labrum and the stability of the hip. Clin Orthop Relat Res 2007;465(465):16–22.

17. Hewitt JD, Glisson RR, Guilak F, Vail TP. The mechanical properties of the human hip capsule ligaments. J Arthroplasty 2002;17(1):82–89.

18. Wagner FV, Negrão JR, Campos J, et al. Capsular ligaments of the hip: anatomic, histologic, and positional study in cadaveric specimens with MR arthrography. Radiology 2012;263(1):189–198.

19. Martin HD, Hatem MA, Kivlan BR, Martin RL. Function of the ligamentum teres in limiting hip rotation: a cadaveric study. Arthroscopy 2014;30(9):1085–1091.

20. Ward WT, Fleisch ID, Ganz R. Anatomy of the iliocapsularis muscle: relevance to surgery of the hip. Clin Orthop Relat Res 2000;(374):278–285.

21. Babst D, Steppacher SD, Ganz R, Siebenrock KA, Tannast M. The iliocapsularis muscle: an important stabilizer in the dysplastic hip. Clin Orthop Relat Res 2011;469(6):1728–1734.

22. Domayer SE, Ziebarth K, Chan J, Bixby S, Mamisch TC, Kim YJ. Femoroacetabular cam-type impingement: diagnostic sensitivity and specificity of radiographic views compared to radial MRI. Eur J Radiol 2011;80(3):805–810.

23. Tannast M, Fritsch S, Zheng G, Siebenrock KA, Steppacher SD. Which radiographic hip parameters do not have to be corrected for pelvic rotation and tilt? Clin Orthop Relat Res 2015;473(4):1255–1266.

24. Siebenrock KA, Kalbermatten DF, Ganz R. Effect of pelvic tilt on acetabular retroversion: a study of pelves from cadavers. Clin Orthop Relat Res 2003;(407):241–248.

25. Tannast M, Mistry S, Steppacher SD, et al. Radiographic analysis of femoroacetabular impingement with Hip2Norm-reliable and validated. J Orthop Res 2008;26(9):1199–1205.

26. Buck FM, Guggenberger R, Koch PP, Pfirrmann CW. Femoral and tibial torsion measurements with 3D models based on low-dose biplanar radiographs in comparison with standard CT measurements. AJR Am J Roentgenol 2012;199(5):W607–W612.

27. Humbert L, Carlioz H, Baudoin A, Skalli W, Mitton D 3rd. 3D Evaluation of the acetabular coverage assessed by biplanar x-rays or single anteroposterior x-ray compared with CT-scan. Comput Methods Biomech Biomed Engin 2008;11(3):257–262.

28. Dawes AR, Seidenberg PH. Sonography of sports injuries of the hip. Sports Health 2014;6(6):531–538.

29. Zbojniewicz AM. US for diagnosis of musculoskeletal conditions in the young athlete: emphasis on dynamic assessment. RadioGraphics 2014;34(5):1145–1162.

30. Sofka CM, Adler RS, Danon MA. Sonography of the acetabular labrum: visualization of labral injuries during intra-articular injections. J Ultrasound Med 2006;25(10):1321–1326.

31. Jin W, Kim KI, Rhyu KH, et al. Sonographic evaluation of anterosuperior hip labral tears with magnetic resonance arthrographic and surgical correlation. J Ultrasound Med 2012;31(3):439–447.

32. Buck FM, Hodler J, Zanetti M, Dora C, Pfirrmann CW. Ultrasound for the evaluation of femoroacetabular impingement of the cam type: diagnostic performance of qualitative criteria and alpha angle measurements. Eur Radiol 2011;21(1):167–175.

33. Byrd JWT, Potts EA, Allison RK, Jones KS. Ultrasound-guided hip injections: a comparative study with fluoroscopy-guided injections. Arthroscopy 2014;30(1):42–46.

34. Lepage-Saucier M, Thiéry C, Larbi A, Lecouvet FE, Vande Berg BC, Omoumi P. Femoroacetabular impingement: normal values of the quantitative morphometric parameters in asymptomatic hips. Eur Radiol 2014;24(7):1707–1714.

35. Tannast M, Kubiak-Langer M, Langlotz F, Puls M, Murphy SB, Siebenrock KA. Noninvasive three-dimensional assessment of femoroacetabular impingement. J Orthop Res 2007;25(1):122–131.

36. Sahin M, Calisir C, Omeroglu H, Inan U, Mutlu F, Kaya T. Evaluation of labral pathology and hip articular cartilage in patients with femoroacetabular impingement (FAI): comparison of multidetector CT arthrography and MR arthrography. Pol J Radiol 2014;79:374–380.

37. Perdikakis E, Karachalios T, Katonis P, Karantanas A. Comparison of MR-arthrography and MDCT-arthrography for detection of labral and articular cartilage hip pathology. Skeletal Radiol 2011;40(11):1441–1447.

38. Petchprapa CN, Dunham KS, Lattanzi R, Recht MP. Demystifying radial imaging of the hip. RadioGraphics 2013;33(3):E97–E112.

39. Rakhra KS, Sheikh AM, Allen D, Beaulé PE. Comparison of MRI alpha angle measurement planes in femoroacetabular impingement. Clin Orthop Relat Res 2009;467(3):660–665.

40. Klenke FM, Hoffmann DB, Cross BJ, Siebenrock KA. Validation of a standardized mapping system of the hip joint for radial MRA sequencing. Skeletal Radiol 2015;44(3):339–343.

41. Pfirrmann CW, Mengiardi B, Dora C, Kalberer F, Zanetti M, Hodler J. Cam and pincer femoroacetabular impingement: characteristic MR arthrographic findings in 50 patients. Radiology 2006;240(3):778–785.

42. Knuesel PR, Pfirrmann CW, Noetzli HP, et al. MR arthrography of the hip: diagnostic performance of a dedicated water-excitation 3D double-echo steady-state sequence to detect cartilage lesions. AJR Am J Roentgenol 2004;183(6):1729–1735.

43. Blankenbaker DG, Ullrick SR, Kijowski R, et al. MR arthrography of the hip: comparison of IDEAL-SPGR volume sequence to standard MR sequences in the detection and grading of cartilage lesions. Radiology 2011;261(3):863–871.

44. Sutter R, Zubler V, Hoffmann A, et al. Hip MRI: how useful is intraarticular contrast material for evaluating surgically proven lesions of the labrum and articular cartilage? AJR Am J Roentgenol 2014;202(1):160–169.

45. Duc SR, Hodler J, Schmid MR, et al. Prospective evaluation of two different injection techniques for MR arthrography of the hip. Eur Radiol 2006;16(2):473–478.

46. Petchprapa CN, Rybak LD, Dunham KS, Lattanzi R, Recht MP. Labral and cartilage abnormalities in young patients with hip pain: accuracy of 3-Tesla indirect MR arthrography. Skeletal Radiol 2015;44(1):97–105.

47. Robinson P. Conventional 3-T MRI and 1.5-T MR arthrography of femoroacetabular impingement. AJR Am J Roentgenol 2012;199(3):509–515.

48. Sundberg TP, Toomayan GA, Major NM. Evaluation of the acetabular labrum at 3.0-T MR imaging compared with 1.5-T MR arthrography: preliminary experience. Radiology 2006;238(2):706–711.

49. Tian CY, Wang JQ, Zheng ZZ, Ren AH. 3.0 T conventional hip MR and hip MR arthrography for the acetabular labral tears

confirmed by arthroscopy. Eur J Radiol 2014;83(10):1822–1827.

50. Rosenberg R, Bernd L, Wrazidlo W, Lederer W, Schneider S. The magnetic resonance tomographic optimization of hip joint cartilage visualization by the selection of a T1-volume gradient-echo sequence and the use of hip-joint traction [in German]. Rofo 1995;163(4):321–329.
51. Llopis E, Cerezal L, Kassarjian A, Higueras V, Fernandez E. Direct MR arthrography of the hip with leg traction: feasibility for assessing articular cartilage. AJR Am J Roentgenol 2008;190(4):1124–1128.
52. Suter A, Dietrich TJ, Maier M, Dora C, Pfirrmann CW. MR findings associated with positive distraction of the hip joint achieved by axial traction. Skeletal Radiol 2015;44(6):787–795.
53. Schmaranzer F, Klauser A, Kogler M, et al. Improving visualization of the central compartment of the hip with direct MR arthrography under axial leg traction: a feasibility study. Acad Radiol 2014;21(10):1240–1247.
54. Schmaranzer F, Klauser A, Kogler M, et al. Diagnostic performance of direct traction MR arthrography of the hip: detection of chondral and labral lesions with arthroscopic comparison. Eur Radiol 2015;25(6):1721–1730.
55. Burgener FA, Kormano M, Pudas T. Bone and joint disorders: differential diagnosis in conventional radiology. Stuttgart, Germany: Thieme, 2006.
56. Bennell KL, Malcolm SA, Thomas SA, Wark JD, Brukner PD. The incidence and distribution of stress fractures in competitive track and field athletes: a twelve-month prospective study. Am J Sports Med 1996;24(2):211–217.
57. Barrack MT, Gibbs JC, De Souza MJ, et al. Higher incidence of bone stress injuries with increasing female athlete triad-related risk factors: a prospective multisite study of exercising girls and women. Am J Sports Med 2014;42(4):949–958.
58. Williams TR, Puckett ML, Denison G, Shin AY, Gorman JD. Acetabular stress fractures in military endurance athletes and recruits: incidence and MRI and scintigraphic findings. Skeletal Radiol 2002;31(5):277–281.
59. Harrast MA, Colonno D. Stress fractures in runners. Clin Sports Med 2010;29(3):399–416.
60. Behrens SB, Deren ME, Matson A, Fadale PD, Monchik KO. Stress fractures of the pelvis and legs in athletes: a review. Sports Health 2013;5(2):165–174.
61. Zingg PO, Buehler TC, Poutawera VR, Alireza A, Dora C. Femoral neck fractures after arthroscopic femoral neck osteochondroplasty for femoroacetabular impingement. Knee Surg Sports Traumatol Arthrosc 2014;22(4):926–931.
62. Matheson GO, Clement DB, McKenzie DC, Taunton JE, Lloyd-Smith DR, MacIntyre JG. Stress fractures in athletes: a study of 320 cases. Am J Sports Med 1987;15(1):46–58.
63. Kiuru MJ, Pihlajamaki HK, Hietanen HJ, Ahovuo JA. MR imaging, bone scintigraphy, and radiography in bone stress injuries of the pelvis and the lower extremity. Acta Radiol 2002;43(2):207–212.
64. Rossi F, Dragoni S. Acute avulsion fractures of the pelvis in adolescent competitive athletes: prevalence, location and sports distribution of 203 cases collected. Skeletal Radiol 2001;30(3):127–131.
65. Nachtrab O, Cassar-Pullicino VN, Lalam R, Tins B, Tyrrell PN, Singh J. Role of MRI in hip fractures, including stress fractures, occult fractures, avulsion fractures. Eur J Radiol 2012;81(12):3813–3823.
66. Dhinsa BS, Jalgaonkar A, Mann B, Butt S, Pollock R. Avulsion fracture of the anterior superior iliac spine: misdiagnosis of a bone tumour. J Orthop Traumatol 2011;12(3):173–176.
67. James SL, Davies AM. Atraumatic avulsion of the lesser trochanter as an indicator of tumour infiltration. Eur Radiol 2006;16(2):512–514.
68. Nepple JJ, Riggs CN, Ross JR, Clohisy JC. Clinical presentation and disease characteristics of femoroacetabular impingement are sex-dependent. J Bone Joint Surg Am 2014;96(20):1683–1689.
69. Leibold MR, Huijbregts PA, Jensen R. Concurrent criterion-related validity of physical examination tests for hip labral lesions: a systematic review. J Manual Manip Ther 2008;16(2):E24–E41.
70. Laborie LB, Lehmann TG, Engesæter IO, Engesæter LB, Rosendahl K. Is a positive femoroacetabular impingement test a common finding in healthy young adults? Clin Orthop Relat Res 2013;471(7):2267–2277.
71. Steppacher SD, Lerch TD, Gharanizadeh K, et al. Size and shape of the lunate surface in different types of pincer impingement: theoretical implications for surgical therapy. Osteoarthritis Cartilage 2014;22(7):951–958.
72. Werner CM, Copeland CE, Ruckstuhl T, et al. Radiographic markers of acetabular retroversion: correlation of the cross-over sign, ischial spine sign and posterior wall sign. Acta Orthop Belg 2010;76(2):166–173.
73. Kappe T, Kocak T, Neuerburg C, Lippacher S, Bieger R, Reichel H. Reliability of radiographic signs for acetabular retroversion. Int Orthop 2011;35(6):817–821.
74. Monazzam S, Agashe M, Hosalkar HS. Reliability of overcoverage parameters with varying morphologic pincer features: comparison of EOS® and radiography. Clin Orthop Relat Res 2013;471(8):2578–2585.
75. Mamisch TC, Zilkens C, Siebenrock KA, Bittersohl B, Kim YJ, Werlen S. MRI of hip osteoarthritis and implications for surgery. Magn Reson Imaging Clin N Am 2010;18(1):111–120.
76. Nepple JJ, Vigdorchik JM, Clohisy JC. What is the association between sports participation and the development of proximal femoral cam deformity? a systematic review and meta-analysis. Am J Sports Med 2015;43(11):2833–2840.
77. Siebenrock KA, Ferner F, Noble PC, Santore RF, Werlen S, Mamisch TC. The cam-type deformity of the proximal femur arises in childhood in response to vigorous sporting activity. Clin Orthop Relat Res 2011;469(11):3229–3240.
78. Chaudhry H, Ayeni OR. The etiology of femoroacetabular impingement: what we know and what we don't. Sports Health 2014;6(2):157–161.
79. Roels P, Agricola R, Oei EH, Weinans H, Campoli G, Zadpoor AA. Mechanical factors explain development of cam-type deformity. Osteoarthritis Cartilage 2014;22(12):2074–2082.
80. Agricola R, Heijboer MP, Ginai AZ, et al. A cam deformity is gradually acquired during skeletal maturation in adolescent and young male soccer players: a prospective study with minimum 2-year follow-up. Am J Sports Med 2014;42(4):798–806.
81. Leunig M, Casillas MM, Hamlet M, et al. Slipped capital femoral epiphysis: early mechanical damage to the acetabular cartilage by a prominent femoral metaphysis. Acta Orthop Scand 2000;71(4):370–375.
82. Murgier J, Reina N, Cavaignac E, Espié A, Bayle-Iniguez X, Chiron P. The frequency of sequelae of slipped upper femoral epiphysis in cam-type femoroacetabular impingement. Bone Joint J 2014;96-B(6):724–729.
83. Albers CE, Steppacher SD, Haefeli PC, et al. Twelve percent of hips with a primary cam deformity exhibit a slip-like morphology resembling sequelae of slipped capital femoral epiphysis. Clin Orthop Relat Res 2015;473(4):1212–1223.
84. Siebenrock KA, Schwab JM. The cam-type deformity: what is it—SCFE, osteophyte, or a new disease? J Pediatr Orthop 2013;33(Suppl 1):S121–S125.
85. Pollard TC, Villar RN, Norton MR, et al. Genetic influences in the aetiology of femoroacetabular impingement: a sibling study. J Bone Joint Surg Br 2010;92(2):209–216.
86. Accadbled F, Pailhé R, Launay F, et al. "Femoroacetabular impingement". Legg-Calve-Perthes disease: from childhood to adulthood. Orthop Traumatol Surg Res 2014;100(6):647–649.
87. Ganz R, Bamert P, Hausner P, Isler B, Vrevc F. Cervico-acetabular impingement after femoral neck fracture [in German]. Unfallchirurg 1991;94(4):172–175.
88. Nötzli HP, Wyss TF, Stoecklin CH, Schmid MR, Treiber K, Hodler J. The contour of the femoral head-neck junction as a predictor for the risk of anterior impingement. J Bone Joint Surg Br 2002;84(4):556–560.
89. Sutter R, Dietrich TJ, Zingg PO, Pfirrmann CW. How useful is the alpha angle for discriminating between symptomatic patients with cam-type femoroacetabular impinge-

ment and asymptomatic volunteers? Radiology 2012;264(2):514–521.

90. Ehrmann C, Rosskopf AB, Pfirrmann CW, Sutter R. Beyond the alpha angle: alternative measurements for quantifying cam-type deformities in femoroacetabular impingement. J Magn Reson Imaging 2015;42(4):1024–1031.

91. Kassarjian A, Yoon LS, Belzile E, Connolly SA, Millis MB, Palmer WE. Triad of MR arthrographic findings in patients with cam-type femoroacetabular impingement. Radiology 2005;236(2):588–592.

92. Frank JM, Harris JD, Erickson BJ, et al. Prevalence of femoroacetabular impingement imaging findings in asymptomatic volunteers: a systematic review. Arthroscopy 2015;31(6): 1199–1204.

93. Sutter R, Pfirrmann CW. Atypical hip impingement. AJR Am J Roentgenol 2013; 201(3):W437–W442.

94. Torriani M, Souto SCL, Thomas BJ, Ouellette H, Bredella MA. Ischiofemoral impingement syndrome: an entity with hip pain and abnormalities of the quadratus femoris muscle. AJR Am J Roentgenol 2009;193(1):186–190.

95. Singer AD, Subhawong TK, Jose J, Tresley J, Clifford PD. Ischiofemoral impingement syndrome: a meta-analysis. Skeletal Radiol 2015;44(6):831–837.

96. Bredella MA, Azevedo DC, Oliveira AL, et al. Pelvic morphology in ischiofemoral impingement. Skeletal Radiol 2015;44(2):249–253.

97. Papavasiliou A, Siatras T, Bintoudi A, et al. The gymnasts' hip and groin: a magnetic resonance imaging study in asymptomatic elite athletes. Skeletal Radiol 2014;43(8):1071–1077.

98. Hetsroni I, Larson CM, Dela Torre K, Zbeda RM, Magennis E, Kelly BT. Anterior inferior iliac spine deformity as an extra-articular source for hip impingement: a series of 10 patients treated with arthroscopic decompression. Arthroscopy 2012;28(11):1644–1653.

99. Gallagher JR. Fracture of the anterior inferior spine of the ileum: sprinter's fracture. Ann Surg 1935;102(1):86–88.

100. Larson CM, Kelly BT, Stone RM. Making a case for anterior inferior iliac spine/subspine hip impingement: three representative case reports and proposed concept. Arthroscopy 2011;27(12):1732–1737.

101. Kolo FC, Charbonnier C, Pfirrmann CW, et al. Extreme hip motion in professional ballet dancers: dynamic and morphological evaluation based on magnetic resonance imaging. Skeletal Radiol 2013;42(5):689–698.

102. Tibor LM, Liebert G, Sutter R, Impellizzeri FM, Leunig M. Two or more impingement and/or instability deformities are often present in patients with hip pain. Clin Orthop Relat Res 2013;471(12):3762–3773.

103. Narvani AA, Tsiridis E, Kendall S, Chaudhuri R, Thomas P. A preliminary report on prevalence of acetabular labrum tears in sports patients with groin pain. Knee Surg Sports Traumatol Arthrosc 2003;11(6):403–408.

104. Byrd JW, Jones KS. Hip arthroscopy in athletes: 10-year follow-up. Am J Sports Med 2009; 37(11):2140–2143.

105. Ranawat AS, Kelly BT. Function of the labrum and management of labral pathology. Oper Tech Orthop 2005;15(3):239–246.

106. Blankenbaker DG, De Smet AA, Keene JS, Fine JP. Classification and localization of acetabular labral tears. Skeletal Radiol 2007;36(5):391–397.

107. Blankenbaker DG, Tuite MJ, Keene JS, del Rio AM. Labral injuries due to iliopsoas impingement: can they be diagnosed on MR arthrography? AJR Am J Roentgenol 2012;199(4): 894–900.

108. Smith CD, Masouros S, Hill AM, Amis AA, Bull AM. A biomechanical basis for tears of the human acetabular labrum. Br J Sports Med 2009;43(8):574–578.

109. Silvis ML, Mosher TJ, Smetana BS, et al. High prevalence of pelvic and hip magnetic resonance imaging findings in asymptomatic collegiate and professional hockey players. Am J Sports Med 2011;39(4):715–721.

110. Gallo RA, Silvis ML, Smetana B, et al. Asymptomatic hip/groin pathology identified on magnetic resonance imaging of professional hockey players: outcomes and playing status at 4 years' follow-up. Arthroscopy 2014;30(10): 1222–1228.

111. Schmitz MR, Campbell SE, Fajardo RS, Kadrmas WR. Identification of acetabular labral pathological changes in asymptomatic volunteers using optimized, noncontrast 1.5-T magnetic resonance imaging. Am J Sports Med 2012;40(6):1337–1341.

112. Register B, Pennock AT, Ho CP, Strickland CD, Lawand A, Philippon MJ. Prevalence of abnormal hip findings in asymptomatic participants: a prospective, blinded study. Am J Sports Med 2012;40(12):2720–2724.

113. Saddik D, Troupis J, Tirman P, O'Donnell J, Howells R. Prevalence and location of acetabular sublabral sulci at hip arthroscopy with retrospective MRI review. AJR Am J Roentgenol 2006;187(5):W507–W511.

114. Studler U, Kalberer F, Leunig M, et al. MR arthrography of the hip: differentiation between an anterior sublabral recess as a normal variant and a labral tear. Radiology 2008; 249(3):947–954.

115. Dinauer PA, Murphy KP, Carroll JF. Sublabral sulcus at the posteroinferior acetabulum: a potential pitfall in MR arthrography diagnosis of acetabular labral tears. AJR Am J Roentgenol 2004;183(6):1745–1753.

116. Kwee RM, Kavanagh EC, Adriaensen ME. Normal anatomical variants of the labrum of the hip at magnetic resonance imaging: a systematic review. Eur Radiol 2013;23(6):1694–1710.

117. Nguyen MS, Kheyfits V, Giordano BD, Dieudonne G, Monu JU. Hip anatomic variants that may mimic abnormalities at MRI: labral variants. AJR Am J Roentgenol 2013;201(3):W394–W400.

118. Weidner J, Büchler L, Beck M. Hip capsule dimensions in patients with femoroacetabular impingement: a pilot study. Clin Orthop Relat Res 2012;470(12):3306–3312.

119. Ganz R, Leunig M, Leunig-Ganz K, Harris WH. The etiology of osteoarthritis of the hip: an integrated mechanical concept. Clin Orthop Relat Res 2008;466(2):264–272.

120. Kaya M, Suzuki T, Emori M, Yamashita T. Hip morphology influences the pattern of articular cartilage damage. Knee Surg Sports Traumatol Arthrosc 2014 Sep 11. [Epub ahead of print]

121. Anderson LA, Peters CL, Park BB, Stoddard GJ, Erickson JA, Crim JR. Acetabular cartilage delamination in femoroacetabular impingement. Risk factors and magnetic resonance imaging diagnosis. J Bone Joint Surg Am 2009;91(2):305–313.

122. Schmid MR, Nötzli HP, Zanetti M, Wyss TF, Hodler J. Cartilage lesions in the hip: diagnostic effectiveness of MR arthrography. Radiology 2003;226(2):382–386.

123. Byrd JW. Lateral impact injury: a source of occult hip pathology. Clin Sports Med 2001;20(4): 801–815.

124. Zaltz I, Leunig M. Parafoveal chondral defects associated with femoroacetabular impingement. Clin Orthop Relat Res 2012;470(12): 3383–3389.

125. Dietrich TJ, Suter A, Pfirrmann CW, Dora C, Fucentese SF, Zanetti M. Supraacetabular fossa (pseudodefect of acetabular cartilage): frequency at MR arthrography and comparison of findings at MR arthrography and arthroscopy. Radiology 2012;263(2):484–491.

126. Vallée C, Chevrot A, Defrance I, Gires F, Wybier M, Pallardy G. Notches of the acetabulum roof: incidence—anatomoradiological correlation [in French]. J Radiol 1988;69(8-9): 533–537.

127. Chang CY, Huang AJ. MR imaging of normal hip anatomy. Magn Reson Imaging Clin N Am 2013;21(1):1–19.

128. Byrd JW. Supraacetabular fossa. Radiology 2012;265(2):648; author reply 648.

129. Bittersohl B, Hosalkar HS, Apprich S, Werlen SA, Siebenrock KA, Mamisch TC. Comparison of pre-operative dGEMRIC imaging with intra-operative findings in femoroacetabular impingement: preliminary findings. Skeletal Radiol 2011;40(5):553–561.

130. Cerezal L, Arnaiz J, Canga A, et al. Emerging topics on the hip: ligamentum teres and hip microinstability. Eur J Radiol 2012;81(12): 3745–3754.

131. Philippon MJ. The role of arthroscopic thermal capsulorrhaphy in the hip. Clin Sports Med 2001;20(4):817–829.

132. Magerkurth O, Jacobson JA, Morag Y, Caoili E, Fessell D, Sekiya JK. Capsular laxity of the hip: findings at magnetic resonance arthrography. Arthroscopy 2013;29(10):1615–1622.

133. Bardakos NV, Villar RN. The ligamentum teres of the adult hip. J Bone Joint Surg Br 2009;91(1):8–15.

134. Shu B, Safran MR. Hip instability: anatomic and clinical considerations of traumatic and atraumatic instability. Clin Sports Med 2011;30(2):349–367.

135. Byrd JW, Jones KS. Traumatic rupture of the ligamentum teres as a source of hip pain. Arthroscopy 2004;20(4):385–391.

136. Gray AJR, Villar RN. The ligamentum teres of the hip: an arthroscopic classification of its pathology. Arthroscopy 1997;13(5):575–578.

137. Cerezal L, Kassarjian A, Canga A, et al. Anatomy, biomechanics, imaging, and management of ligamentum teres injuries. RadioGraphics 2010;30(6):1637–1651.

138. Sampatchalit S, Barbosa D, Gentili A, Haghighi P, Trudell D, Resnick D. Degenerative changes in the ligamentum teres of the hip: cadaveric study with magnetic resonance arthrography, anatomical inspection, and histologic examination. J Comput Assist Tomogr 2009;33(6):927–933.

139. Datir A, Xing M, Kang J, et al. Diagnostic utility of MRI and MR arthrography for detection of ligamentum teres tears: a retrospective analysis of 187 patients with hip pain. AJR Am J Roentgenol 2014;203(2):418–423.

140. Petchprapa CN, Bencardino JT. Tendon injuries of the hip. Magn Reson Imaging Clin N Am 2013;21(1):75–96.

141. Mulligan EP, Middleton EF, Brunette M. Evaluation and management of greater trochanter pain syndrome. Phys Ther Sport 2015;16(3):205–214.

142. Kong A, Van der Vliet A, Zadow S. MRI and US of gluteal tendinopathy in greater trochanteric pain syndrome. Eur Radiol 2007;17(7):1772–1783.

143. Lewis CL. Extra-articular snapping hip: a literature review. Sports Health 2010;2(3):186–190.

144. Lee KS, Rosas HG, Phancao JP. Snapping hip: imaging and treatment. Semin Musculoskelet Radiol 2013;17(3):286–294.

145. Choi YS, Lee SM, Song BY, Paik SH, Yoon YK. Dynamic sonography of external snapping hip syndrome. J Ultrasound Med 2002;21(7):753–758.

146. Mellado JM, Bencardino JT. Morel-Lavallée lesion: review with emphasis on MR imaging. Magn Reson Imaging Clin N Am 2005;13(4):775–782.

147. Nickerson TP, Zielinski MD, Jenkins DH, Schiller HJ. The Mayo Clinic experience with Morel-Lavallée lesions: establishment of a practice management guideline. J Trauma Acute Care Surg 2014;76(2):493–497.

148. Kalaci A, Karazincir S, Yanat AN. Long-standing Morel-Lavallée lesion of the thigh simulating a neoplasm. Clin Imaging 2007;31(4):287–291.

149. Deslandes M, Guillin R, Cardinal E, Hobden R, Bureau NJ. The snapping iliopsoas tendon: new mechanisms using dynamic sonography. AJR Am J Roentgenol 2008;190(3):576–581.

150. Pelsser V, Cardinal E, Hobden R, Aubin B, Lafortune M. Extraarticular snapping hip: sonographic findings. AJR Am J Roentgenol 2001;176(1):67–73.

151. Bui KL, Ilaslan H, Recht M, Sundaram M. Iliopsoas injury: an MRI study of patterns and prevalence correlated with clinical findings. Skeletal Radiol 2008;37(3):245–249.

152. Shabshin N, Rosenberg ZS, Cavalcanti CFA. MR imaging of iliopsoas musculotendinous injuries. Magn Reson Imaging Clin N Am 2005;13(4):705–716.

153. Agten CA, Rosskopf AB, Zingg PO, Peterson CK, Pfirrmann CW. Outcomes after fluoroscopy-guided iliopsoas bursa injection for suspected iliopsoas tendinopathy. Eur Radiol 2015;25(3):865–871.

154. Blankenbaker DG, De Smet AA, Keene JS. Sonography of the iliopsoas tendon and injection of the iliopsoas bursa for diagnosis and management of the painful snapping hip. Skeletal Radiol 2006;35(8):565–571.

155. Lecouvet FE, Demondion X, Leemrijse T, Vande Berg BC, Devogelaer J-P, Malghem J. Spontaneous rupture of the distal iliopsoas tendon: clinical and imaging findings, with anatomic correlations. Eur Radiol 2005;15(11):2341–2346.

156. Hasselman CT, Best TM, Hughes C 4th, Martinez S, Garrett WE Jr. An explanation for various rectus femoris strain injuries using previously undescribed muscle architecture. Am J Sports Med 1995;23(4):493–499.

157. Kassarjian A, Rodrigo RM, Santisteban JM. Current concepts in MRI of rectus femoris musculotendinous (myotendinous) and myofascial injuries in elite athletes. Eur J Radiol 2012;81(12):3763–3771.

158. Gyftopoulos S, Rosenberg ZS, Schweitzer ME, Bordalo-Rodrigues M. Normal anatomy and strains of the deep musculotendinous junction of the proximal rectus femoris: MRI features. AJR Am J Roentgenol 2008;190(3):W182–W186.

159. Beltran L, Ghazikhanian V, Padron M, Beltran J. The proximal hamstring muscle-tendon-bone unit: a review of the normal anatomy, biomechanics, and pathophysiology. Eur J Radiol 2012;81(12):3772–3779.

160. Ekstrand J, Hägglund M, Waldén M. Injury incidence and injury patterns in professional football: the UEFA injury study. Br J Sports Med 2011;45(7):553–558.

161. Ekstrand J, Healy JC, Waldén M, Lee JC, English B, Hägglund M. Hamstring muscle injuries in professional football: the correlation of MRI findings with return to play. Br J Sports Med 2012;46(2):112–117.

162. Pollock N, James SL, Lee JC, Chakraverty R. British athletics muscle injury classification: a new grading system. Br J Sports Med 2014;48(18):1347–1351.

163. De Smet AA, Best TM. MR imaging of the distribution and location of acute hamstring injuries in athletes. AJR Am J Roentgenol 2000;174(2):393–399.

164. De Smet AA, Blankenbaker DG, Alsheik NH, Lindstrom MJ. MRI appearance of the proximal hamstring tendons in patients with and without symptomatic proximal hamstring tendinopathy. AJR Am J Roentgenol 2012;198(2):418–422.

165. Bierry G, Simeone FJ, Borg-Stein JP, Clavert P, Palmer WE. Sacrotuberous ligament: relationship to normal, torn, and retracted hamstring tendons on MR images. Radiology 2014;271(1):162–171.

166. Bowman KF Jr, Cohen SB, Bradley JP. Operative management of partial-thickness tears of the proximal hamstring muscles in athletes. Am J Sports Med 2013;41(6):1363–1371.

167. Meyers WC, Foley DP, Garrett WE, Lohnes JH, Mandlebaum BR; PAIN (Performing Athletes with Abdominal or Inguinal Neuromuscular Pain) Study Group. Management of severe lower abdominal or inguinal pain in high-performance athletes. Am J Sports Med 2000;28(1):2–8.

168. Mullens FE, Zoga AC, Morrison WB, Meyers WC. Review of MRI technique and imaging findings in athletic pubalgia and the "sports hernia". Eur J Radiol 2012;81(12):3780–3792.

169. Zoga AC, Kavanagh EC, Omar IM, et al. Athletic pubalgia and the "sports hernia": MR imaging findings. Radiology 2008;247(3):797–807.

170. Brennan D, O'Connell MJ, Ryan M, et al. Secondary cleft sign as a marker of injury in athletes with groin pain: MR image appearance and interpretation. Radiology 2005;235(1):162–167.

171. Coker DJ, Zoga AC. The role of magnetic resonance imaging in athletic pubalgia and core muscle injury. Top Magn Reson Imaging 2015;24(4):183–191.

172. Murphy G, Foran P, Murphy D, Tobin O, Moynagh M, Eustace S. "Superior cleft sign" as a marker of rectus abdominus/adductor longus tear in patients with suspected sportsman's hernia. Skeletal Radiol 2013;42(6):819–825.

173. Omar IM, Zoga AC, Kavanagh EC, et al. Athletic pubalgia and "sports hernia": optimal MR imaging technique and findings. RadioGraphics 2008;28(5):1415–1438.

174. Drakos MC, Domb B, Starkey C, Callahan L, Allen AA. Injury in the national basketball association: a 17-year overview. Sports Health 2010;2(4):284–290.

175. Agel J, Dompier TP, Dick R, Marshall SW. Descriptive epidemiology of collegiate men's ice hockey injuries: National Collegiate Athletic Association Injury Surveillance System, 1988-1989 through 2003-2004. J Athl Train 2007;42(2):241–248.

176. McKay CD, Tufts RJ, Shaffer B, Meeuwisse WH. The epidemiology of professional ice hockey injuries: a prospective report of six NHL seasons. Br J Sports Med 2014;48(1):57–62.